Reviewed Preprint
v1 • November 11, 2025
Not revised

Reviewed Preprint
v2 • June 2, 2026
Revised by authors

For correspondence:
coeno@arizona.edu

Competing interests: No competing interests declared

Funding: See page 24

Reviewing editor: Benjamin L Parker, The University of Melbourne, Australia

The titin N2A-MARP signalosome constrains muscle longitudinal hypertrophy in response to stretch

Robbert van der Pijl[1,2], Jochen Gohlke[1], Joshua Strom[1], Eva Peters[1], Shengyi Shen[1], Stefan Conijn[2], Zaynab Hourani[1], Stephan Lange[3,4], Ju Chen[3], Paul Langlais[5], Siegfried Labeit[6], Henk Granzier[1], Coen Ottenheijm[1,2]

[1]Department of Cellular and Molecular Medicine, University of Arizona, Tucson, United States • [2]Department of Physiology, Amsterdam University Medical Center, location VUMC, Amsterdam, Netherlands • [3]School of Medicine, University of California, San Diego, San Diego, United States • [4]Department of Biomedicine, Aarhus University, Aarhus, Denmark • [5]Department of Endocrinology, University of Arizona, Tucson, United States • [6]Department of Integrative Pathophysiology, Medical Faculty Mannheim, Mannheim, Germany

eLife Assessment

The work by van der Pijl presents **important** findings on the role of titin-associated muscle ankyrin repeat proteins (MARPs) on hypertrophy via mTOR signalling. The study presents rigourous data using in vivo loss-of-function and pharmacological approaches to investigate effects on hypertrophy. While the evidence supporting the role of MARPs on hypertrophy is **solid**, there are limitations. For example, the use of Rapamycin only inhibits some aspects of mTORC1 signalling and the study is limited to analysis of the diaphragm and thus it is not clear if the mechanisms are conserved across other muscle types.

https://doi.org/10.7554/eLife.107597.2.sa3

Abstract

Titin-based mechanosensing is a key driver of trophic signaling in muscle, yet the downstream pathways linking titin sensing to muscle remodeling remain poorly understood. To investigate these signaling mechanisms, we utilized unilateral diaphragm denervation (UDD), an in vivo model that induces titin-stiffness-dependent hypertrophy via mechanical stretch. Using UDD in rats and mice, we characterized the longitudinal hypertrophic response and distinguished stretch-induced signaling from denervation effects by performing global transcriptomic and proteomic analyses following UDD and bilateral diaphragm denervation (BDD) in rats. Our findings identified upregulation of titin-associated muscle ankyrin repeat proteins (MARPs). Subsequent phosphorylation enrichment mass spectrometry in mouse diaphragm highlighted the involvement of the N2A-element. UDD in MARP knockout (KO) mice resulted in enhanced longitudinal hypertrophy, with Western blot analysis revealing activation of the mTOR pathway. Furthermore, pharmacological inhibition of mTORC1 with rapamycin suppressed longitudinal hypertrophy, demonstrating that mTOR signaling regulates titin-mediated hypertrophic growth in a MARP-dependent manner. These findings establish MARPs as key modulators of titin-based mechanotransduction and highlight mTORC1 as a central regulator of longitudinal muscle hypertrophy.

Introduction

Titin is a giant protein in striated muscle and forms an elastic filament in sarcomeres[1], the smallest contractile unit in muscle. One of the functions attributed to titin is to generate passive tension in muscle[2,3], ensuring optimal overlap of the actin-based thin filaments and myosin-based thick filaments for muscle contraction. The elastic properties of titin combined with its arrangement in the sarcomeres, spanning the half-sarcomere, make titin an ideal stress sensor. The mechanosensory properties of titin have been extensively described[4–6] and appear to localize to several signaling hotspots on titin.

In skeletal muscle, the N2A element is the prevalent titin region associated with hypertrophy signaling. The N2A element is known for its interaction with the muscle ankyrin repeat proteins (MARP1-3)[7,8] and calpain3[9]. All MARPs have been implicated in trophicity signaling, with redundancy between the MARP proteins[7,10]. MARP1 tethers titin to the thin filament, forming a mechanism for increasing passive tension[11,12]. In the heart, MARP1 also interacts with MLP and protein kinase C alpha in intercalated disks, resulting in a maladaptive trophic response in dilated cardiomyopathy[10]. MARP2 can be phosphorylated at serine-99 (S69 in mice) by Akt, resulting in reduced differentiation potential of myoblasts[13]. MARP2 has also been linked to the NFkB-pathway in inflammatory responses[14], suggesting MARP2 may have roles in atrophy signaling. MARP3 is the least studied member of the MARPs but appears to play a role in glucose uptake and vascular remodeling in skeletal muscle[15,16]. Titin has previously been shown to activate signaling in response to stretch[17,18], providing a potential activation mechanism for N2A to activate trophic signaling.

Muscle hypertrophy is directly associated with titin-based stiffness. High stiffness, as observed in the $Ttn^{\Delta ex112–158}$ and $Ttn^{\Delta ex219-225}$ mouse models[19,20], results in longitudinal hypertrophy, i.e. an increase in serial-linked sarcomeres, to reduce sarcomere length and normalize passive tension. We previously used a surgical model in which we denervated one hemi-diaphragm (unilateral diaphragm denervation, UDD)[21], inducing passive cyclic stretch of the denervated hemi-diaphragm by the innervated costal to induce (longitudinal) hypertrophy. This hypertrophy was dependent on titin-based stiffness, as higher titin stiffness resulted in exaggerated hypertrophy and lower titin stiffness resulted in attenuated hypertrophy[21]. UDD is a unique model as it allows the *in vivo* study of passive stretch-induced muscle hypertrophy.

We used UDD as a model for studying titin-mechanosensing and examined the signaling that underlies the hypertrophy response. Our findings support the N2A-MARP signalosome inhibiting longitudinal hypertrophy and show mTOR signaling to be a prominent contributor to longitudinal hypertrophy.

Results

Longitudinal hypertrophy regulates transient trophicity in UDD

A unique aspect of unilateral diaphragm denervation (UDD) is the transient nature of the hypertrophy. This transient nature is likely the result from changes in fractional extension of sarcomeres. Sarcomere length (SL) at end-expiration length was 2.9±0.1 µm in sham, while stretch lengths at end-inspiration were predicted to reach 3.7 µm directly after denervation of the right costal diaphragm (Figure 1A, previously published[21]). Such sarcomere lengths put high strain on titin (Figure 1A, right panel), providing a potent trigger for mechanosensing and subsequent hypertrophy signaling. Our results show that during 6-days of UDD the denervated costal rapidly hypertrophies, followed by slow onset of atrophy (Figure 1B). The mass increase coincides with longitudinal hypertrophy of muscle fibers, addition of serial-linked sarcomeres, adding 952±81 sarcomeres (30.2% increase in total fiber length; $p<0.0001$; Figure 1C) following 6-days of UDD. This increase in sarcomere number appeared to stabilize by 6-days UDD, as at 12-day UDD sarcomere addition was measured to be 778±87 sarcomeres versus sham levels (not significantly different compared to 6-day UDD). Assuming that fractional extension of sarcomeres during inspiration decreases with longitudinal hypertrophy, 30.2% increase in sarcomere number would

reduce the sarcomere length at end inspiration from 3.7 µm to ~2.8 µm, in close agreement with whole body formaldehyde perfusion experiments which showed sarcomere lengths of 2.7±0.1 µm[21]. As a SL of 2.8 µm falls below the end-expiration SL, the denervated costal effectively no longer experiences "stretch", reducing titin's mechanosensing trigger and thus explaining the transient nature of the hypertrophy seen in UDD.

To confirm that stretch is the trigger for hypertrophy, rather than denervation, we performed bilateral diaphragm denervation in rats (BDD), resulting in complete inactivity of the diaphragm. Note that we attempted BDD in mice but experienced high mortality rates, while survival in rat was >75%. All rats were of similar body weight pre-surgery and showed a slight decrease in body weight after 3-day BDD (Supplemental Figure 1A; p=0.036), and comparable tibial length and soleus weights (Supplemental Figure 1B & C). Similar to mice, rats present with increased denervated costal mass after 3-day UDD: 14.68±0.64 mg/mm versus sham rats 10.82±0.39 mg/mm (Figure 1D; p>0.0001; muscle weight normalized to tibial length). However, 3-day BDD rats did not develop increased mass 11.92±0.89 mg/mm compared to sham rats 10.82±0.39 mg/mm. The increase in costal mass at 3-day UDD results in part from an increase in longitudinal hypertrophy, with denervated costal diaphragm adding 933±301 serial sarcomeres compared to sham animals (Figure 1E; p=0.018), whereas 3-day BDD rats showed no difference in serial sarcomere number (7559±313 versus sham 7740±111). Thus, stretch and not denervation triggers longitudinal hypertrophy.

To support titin's role as mechanosensor of stretch to drive hypertrophy, we performed RNAseq on both UDD and BDD operated rat diaphragms. Splicing appears mostly unaffected in UDD animals, while BDD rats showed marked increased splicing in exons encoding the elastic PEVK region of titin suggesting reduced titin compliance (Supplemental Figure 2). To study how titin compliance might affect the hypertrophy response in UDD, we performed UDD on Rbm20$^{\Delta RRM}$ mice and Rbm20 ko rats. Rbm20 is an RNA splicing-factor for titin and both the mouse and rat model generate larger, more compliant titin isoforms and should thus be less sensitive to stretch. Rbm20$^{\Delta RRM}$ mice showed relatively less tissue mass increase compared to wildtype (WT) 3, 6, or 12-days UDD (Supplemental Figure 3A), without changes in longitudinal hypertrophy at 6-days UDD (Supplemental Figure 3B) suggesting the difference in mass is a result from radial fiber growth, in agreement with our previous findings[21]. Finally, we compared denervated costal mass from Sprague Dawley (SD) and Rbm20 ko rats 3-day UDD, showing a difference in mass increase of 24.4±3.8% in Rbm20 ko and 35.5±5.9% in SD rats (p=0.02; Supplemental Figure 3C), supporting that stretch evokes hypertrophy in muscle and that titin compliance modulates the extent of hypertrophy across species. Thus, muscle stretch in the costal diaphragm is a potent trigger for longitudinal muscle hypertrophy, with titin being a primary sensor.

Global transcriptome and proteome level studies reveal a distinct subset of genes and proteins involved in UDD stretch hypertrophy

To identify the cellular processes involved in stretch-based hypertrophy we performed both transcriptome wide studies by RNA sequencing (RNAseq) as well as proteome studies by global mass spectrometry (MS) on our rat 3-day sham, UDD and BDD samples. Initial studies focused on separating the effect of denervation versus stretch. Principal component analysis of the top 500 genes showed close clustering of samples by group (Supplemental Figure 4A), suggesting distinct gene programs are active between sham, UDD and BDD. At the protein level, principal component analysis of the top 250 proteins suggests narrow separation of groups, predicting overlap of the BDD and UDD samples (Supplemental Figure 4B). Gene expression studies revealed very close overlap of BDD and UDD profiles with 77.15% overlap in differentially expressed genes (DEG's: p_{adj}<0.05) and just 9.4% of DEG's being specific for UDD (Figure 2A). Volcano plots of UDD>Sham (Figure 2B, left panel) and BDD>Sham (Figure 2B; middle panel) showed the ~11.000 DEG's (Supplemental data Tables 1-6) to be nearly equally distributed between up and downregulated DEG's. Direct comparison of UDD>BDD (Figure 2B, right panel) revealed 850 DEG's to be uniquely associated with UDD, of which 581 were upregulated (Supplemental data Table 3). MS studies broadly agreed with the RNAseq data, showing UDD and BDD share overlapping

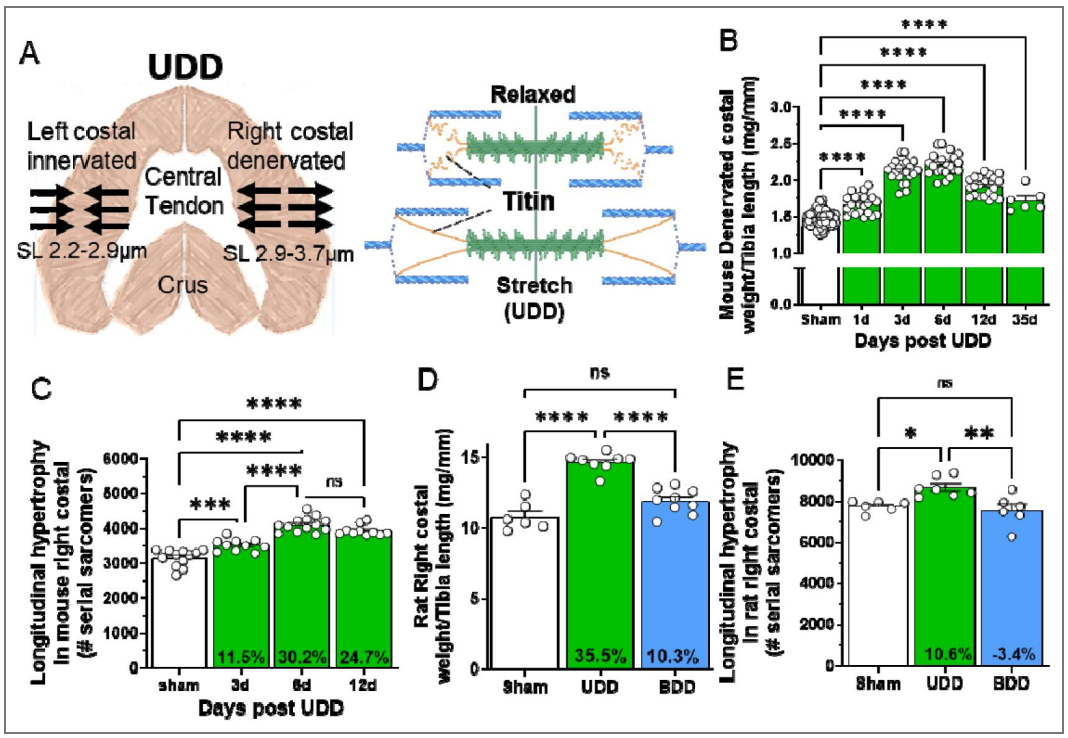

Figure 1. Transient hypertrophy following UDD in the denervated costal diaphragm.

(A) schematic of how UDD affects sarcomere length in the denervated costal (left panel) and how stretch extends titin for mechanosensing (right panel, generated using *BioRender.com*). (B) Mouse diaphragm costal weight normalized to tibial length following 1, 3, 6, 12 and 35-days of UDD, showing the hypertrophy phase peaking at 6-days and progressing to the atrophy phase at 12-days post-UDD (n=6-22, shams grouped for simplicity). A substantial part of the hypertrophy seen in mice encompasses longitudinal hypertrophy (C), lengthening of the muscle fibers by addition of serial sarcomeres (n=10-13). The increased fiber length likely reduces the stretch-based hypertrophy signaling and thus explains the transient nature of hypertrophy. (D) 3-day BDD in rats (n=6-9) confirms stretch is the trigger for inducing hypertrophy in UDD at the tissue mass level (D; rat diaphragm right costal normalized to tibial length, denervated in UDD) and serial sarcomeres level (E). One-way ANOVA, with Tukey post-hoc testing.

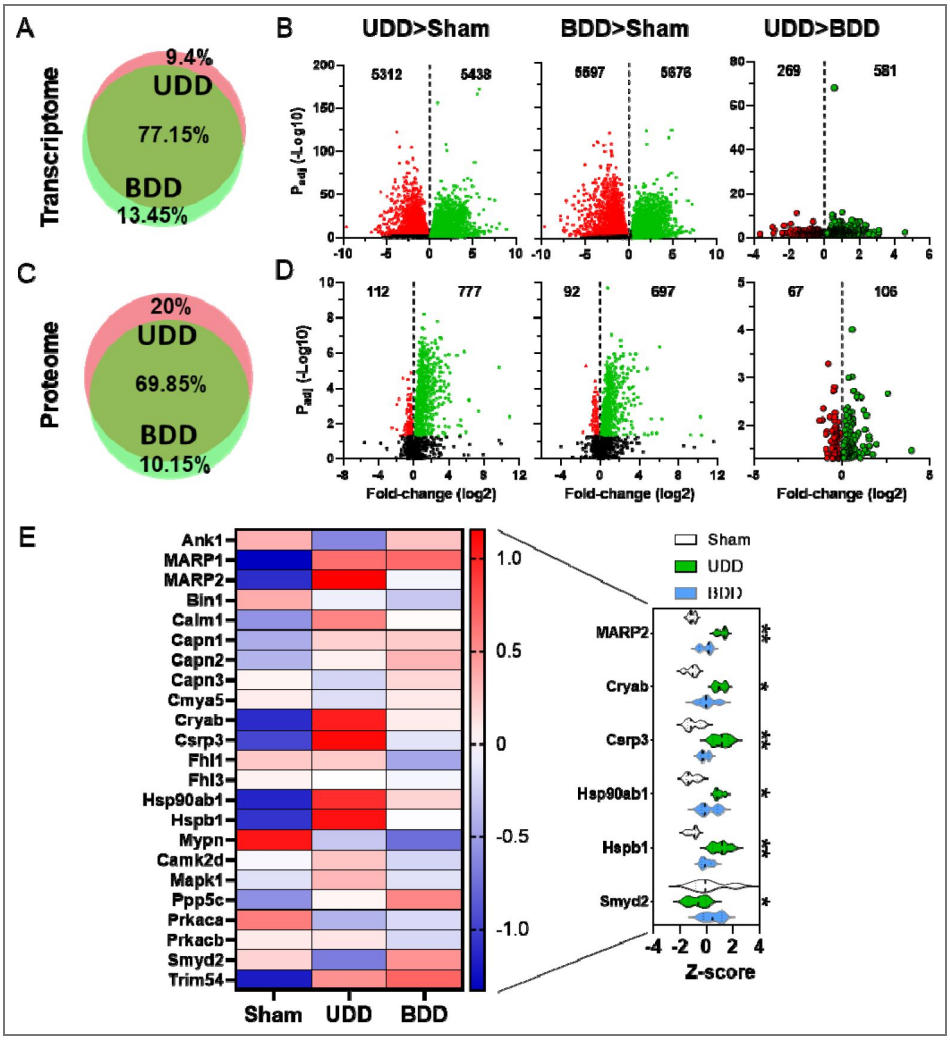

Figure 2. Global transcriptomics and proteomics following 3-days UDD and BDD in rats.

Global transcript studies by RNAseq of sham, UDD and BDD right costal diaphragm (n=5/group). Same parameters apply to the global proteome studies (C-D) with mass spectrometry. Quantitative Venn diagrams of the transcriptome (A) showing overlap gene regulation between UDD and BDD. Vulcano plots of UDD (B, left) and BDD (B, middle) showed similar gene regulation. Comparing UDD to BDD directly revealed just 850 differentiall regulated genes (B, right) indicating a small subset being responsible for hypertrophy regulation. Quantitative Venn diagrams of the proteome (C) showed similar regulation compared to transcriptome. Volcano plots of UDD (D, left) and BDD (D, middle) showed primarily upregulation of proteins. Comparing UDD to BDD directly revealed just 173 differentiall regulated proteins (D, right). Green-dots: upregulated genes/proteins, red-dots: downregulated genes/proteins. Titin-associated proteins in heatmap of proteome (E; Z-score: red= upregulated, blue= downregulated) and violin plots (right panel) of differential proteins between UDD (red) and BDD (blue), indicating upregulation of titin-associate proteins following stretch. 2-way ANOVA (sham vs UDD and sham vs BDD) p_{int}: *p<0.05, **P<0.01.

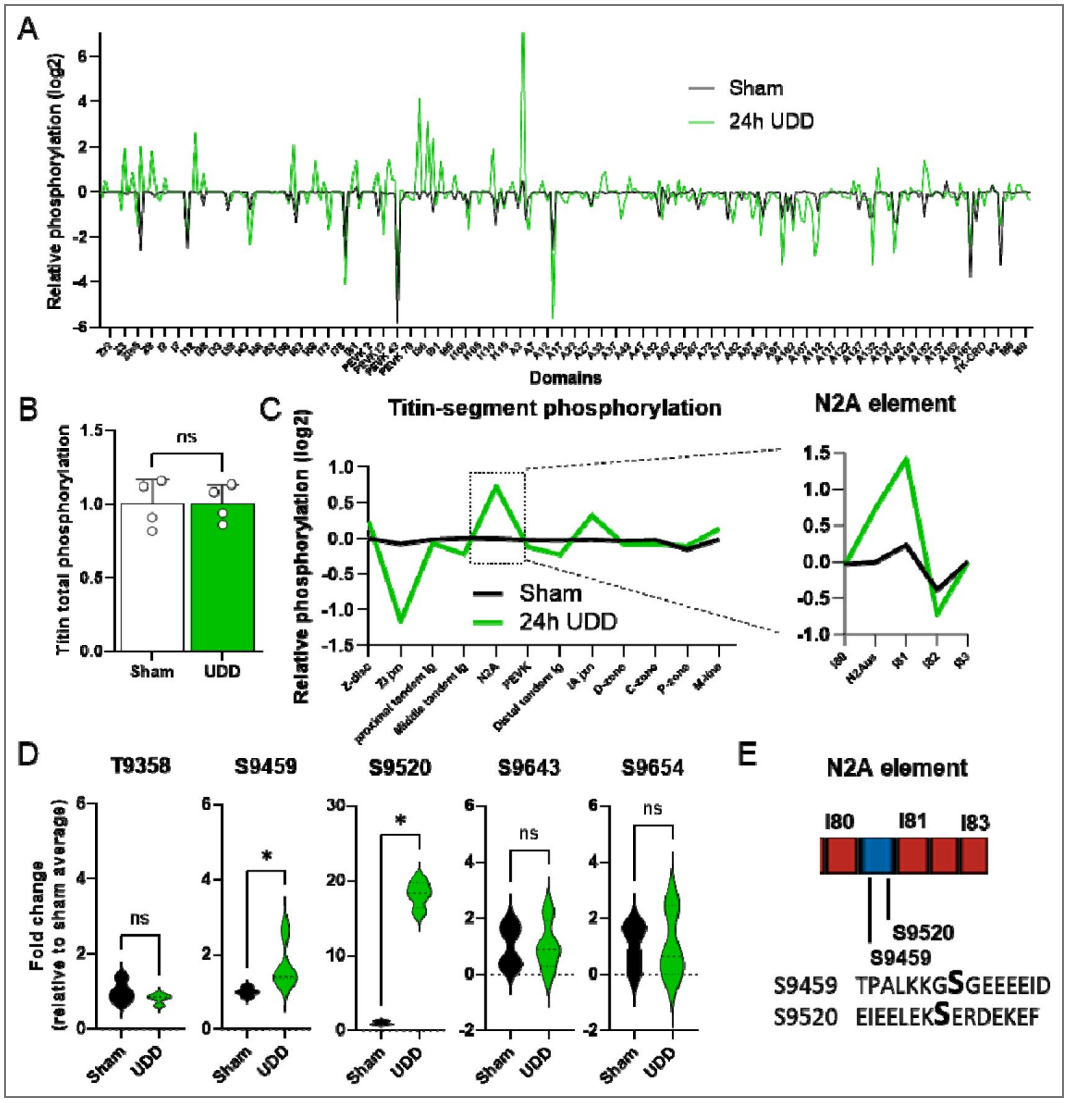

Figure 3. Phosphorylation of titin following 24-hours of UDD by mass spectrometry (n=4/group).

Phosphorylation of individual titin domains (A) relative Z-score (log2) of titin phosphorylation showing domain specific changes in phosphorylation. Total phosphorylation of titin (B) is not affected by UDD, however titin showed regional changes in phosphorylation (C), notably increased phosphorylation of the N2A-element (boxed). Fold-change of the phosphorylation signal for the 5 main sites found in the N2A-element (D). (E) Schematic of the N2A element with the 2 pSer found in the N2Aus (Transcript: ENSMUST00000099981.10 Ttn-203). Red: Ig domain coding and blue: unique sequence coding. Mouse titin phosphorylation and global mass spectrometry was analyzed by t-test, Kolmogorov-Smirnov test or multiple t-test with a cut-off at P<0.05.

expression programs (Figure 2A & C). Twenty percent of the differentially expressed proteins (DEP's; P<0.05) detected are unique to UDD (Figure 2C). Volcano plots of UDD>Sham (Figure 2D, left panel) and BDD>Sham (Figure 2D, middle panel) showed 889 and 789 DEP's, respectively, (Supplemental data Tables 7-12) which were primarily increased. Comparing UDD>BDD revealed 173 DEP's (Figure 2D, right panel) that are unique to UDD. Most of DEP's (and DEG's) found are related to transcription, translation, energetics and folding, with the highest fold DEP's in rat UDD>BDD being: Med15 (15.5-fold), Eif3i (6.0-fold) and Gtpbp3 (3.9-fold) (Supplemental data Table 9). GOterm enrichment of UDD>BDD, separated by downregulated and upregulated DEG's (Supplemental Figure 3C, left top and bottom graph, respectively), and DEP's (Supplemental Figure 4C, right top and bottom graph, respectively), indicated that upregulated DEG/DEP's are primarily related to muscle development and function consistent with an active hypertrophy program and downregulated targets with metabolism and cellular respiration. Concurrently, KEGG PATHWAY database searches (Supplemental data Table 6) indicated that the DEG's are involved in muscle remodeling. Thus, UDD has a expression profile that is distinct from denervation (BDD), with more focus on remodeling of muscle.

Exploring if titin-mechanosensing was active in either UDD or BDD we generated heatmaps of titin-binding proteins based on RNAseq (Supplemental Figure 5) and global MS data (Figure 2E). To narrow down proteins that were differential between UDD and BDD we tested (2-way ANOVA p_{int}<0.1) the z-score and found: MARP2 (Ankrd2; p=0.003), Cryab (p= 0.026), Csrp3 (p= 0.002), Hsp90ab1 (p= 0.09), Hspb1 (p= 0.008) and Smyd2 (p= 0.004), to be unique to UDD. Interestingly, these DEP's (MARP2, Smyd2, Hsp1b, Hsp90ab and Cryab) are established binding partners of the N2A element of titin.[22]

Titin phosphorylation in UDD

With the rat data indicating changes in titin-associated signaling and titin stiffness modifying the hypertrophy response in mice, we evaluated how UDD affects titin post-translationally. We performed MS on phosphorylation enriched peptides from 24-hour UDD diaphragm samples. 24-hour UDD was selected to study the early phosphorylation events. MS revealed 2870 phosphorylated peptides (p<0.05), of which 142-sites were in titin (~700-sites identified including non-significant sites; Supplemental data Table 13). We opted to define titin phosphorylation by analyzing the phosphorylation at the domain level to study if titin showed regional changes in phosphorylation (Figure 3A and Supplemental data Table 14), as total titin phosphorylation (Figure 3B) was unchanged. Domain level analysis indicated titin phosphorylation was primarily changing in the I-band. This motivated quantifying titin phosphorylation by segment (Figure 3C and Supplemental data Table 15; following established naming conventions in Kolmerer and Labeit[1], and Bang et al[23]). Segmental analysis of titin (Figure 3C) revealed a marked increase in phosphorylation of the N2A-element and I/A-junction, and a decrease in the Z/I-junction. Focusing on the increase in phosphorylation of the N2A-element, a known trophicity signaling hub (reviewed in [22]), we assessed the specific domain phosphorylation of the N2A-element (Figure 3C, highlight). In the N2A-element we found 7 phosphorylation sites (Figure 3D-E) of which S9346 & S9350 are located in a linker sequence between I79 and I80, S9483 in I80, S9459 & S9520 in the N2A unique sequence, S9654 in I81 and S9643 in I82). The 2 sites located in the N2A unique sequence were significantly upregulated following UDD (Figure 3D-E). pS9459 and pS9520 currently have no known function but could serve as a recruitment signal (see discussion).

The MARP proteins regulate hypertrophy in UDD

The MARP1 and MARP2 proteins were strongly expressed both at the RNA level and protein level following UDD (Figure 2E). MARPs have been shown to be important regulators of trophicity and have been proposed as intermediaries between titin and trophic signaling pathways (see discussion). As the MARPs share high homology and possible redundancy[7], we performed 6-day UDD on both single- and multi-KO combinations of the MARPs. We initially performed UDD on the MARP triple KO mice (MARP tKO; knockout of Ankrd1, -2 and -23 genes) and found a 12%

reduction in the hypertrophy response compared to WT (Figure 4A; p=0.0099). This reduction in hypertrophy supports a potential link between titin-mechanosensing and MARP-based trophic signaling. To test if one or a combination of MARPs caused the reduction in hypertrophy, we performed 6-day UDD on MARP1 (Ankrd1), MARP2 (Ankrd2) and MARP3 (Ankrd23) KO mice (Figure 4B-D) and double KO for MARP1/2, MARP1/3 and MARP2/3 (Supplemental Figure 6). Whereas MARP1 KO mice did not show a difference in denervated costal diaphragm mass, MARP2 KO mice showed a 14% increase (p=0.003) in mass and MARP3 KO mice showed a 13% reduction (p=0.004) in mass gain. However, all MARP double KO mice also presented with attenuated hypertrophy (Supplemental Figure 6). This suggests that the separate MARP proteins could have distinct functions in UDD, and there may be a dependency for two MARPs in regulating trophic signaling, further discussed in the discussion section.

MARPs negatively regulate longitudinal hypertrophy

Prompted by the reduction in diaphragm mass gain during UDD in MARP tKO mice and by the complexity of targeting all the single MARP KOs, we assessed longitudinal hypertrophy in 6-day UDD MARP tKO samples. MARP tKO mice at baseline have fewer serial sarcomeres than WT (2476±55 vs. 3157±69, respectively; p<0.0001), however 6-days UDD MARP tKO had similar numbers of sarcomeres to WT, 4081±44 versus 4109±59 (Figure 5A). These data show MARP tKO mice add 653 ± 91.6 more sarcomeres than wildtype mice (Figure 5B; 1605±71 vs. 952±59, respectively; p<0.0001). To discern a possible mechanism of the MARPs inhibiting longitudinal hypertrophy, we probed several candidate proteins of hypertrophy pathways that were prominent in the MS datasets. Western blots for MAPK1/3, Calcineurin, mTOR, P70 S6K and 4E-BP1 were performed on costal diaphragms of WT and MARP tKO, 6-day Sham and UDD animals. All samples were normalized to Gapdh and data were presented as relative to WT sham (Figure 5C; representative western blot images in Figure 5D). Mapk1 showed increases in protein level that were comparable between WT and MARP tKO, whereas MAPK3 showed preferential upregulation in MARP tKO (p= 0.0099). Calcineurin was unchanged following UDD, note that in a t-test the WT mice showed a significant increase in UDD. In WT mice, mTor showed a striking increase in expression following 6-day UDD (p= 0.0006), whereas in MARP tKO this was trending (P= 0.08). Downstream proteins of mTORC1; P70 S6K and 4E-BP1 both showed altered regulation, with P70 S6K being similarly upregulated in WT (p= 0.0005) versus MARP tKO (p= 0.001), while 4E-bp1 was only significantly upregulated in MARP tKO (p= 0.033). 2way-ANOVA for the signaling proteins did not indicate specific pathway changes between WT and MARP tKO.

mTOR signaling regulates longitudinal hypertrophy in UDD

Motivated by the data from the mTor western blots in the MARP tKO mice and mTor being a prominent regulator of skeletal muscle hypertrophy, we performed UDD in WT mice treated with rapamycin, an inhibitor of mTORC1 signaling and skeletal muscle hypertrophy. The rat transcriptome studies also indicated calcium signaling (Supplemental data Table 6) to be a prominent pathway in UDD. To test the role of calcium signaling we included a second inhibitor; cyclosporin A, an inhibitor of the calcineurin-NFAT pathway, another hypertrophy regulating pathway. Mice received twice daily intraperitoneal injections of either rapamycin (2.5 mg/kg/day), cyclosporin A (25 mg/kg/day) or vehicle (DMSO), starting 3-days prior to surgery until sacrifice of the mice (schematic in Figure 6A). Cyclosporin A treated mice did not show a change in hypertrophy (Figure 6B) or serial sarcomere addition (Figure 6C), indicating that the calcineurin-NFAT pathway is not a primary mechanism for hypertrophy in UDD. Treatment did not affect the innervated left costal diaphragm (Figure 6D), body weight (Figure 6E) or tibia length (Figure 6F). Interestingly, mice that received rapamycin displayed less hypertrophy of the denervated costal diaphragm (Figure 6B; - 11.2%; p<0.001) compared to vehicle treated mice. This attenuated hypertrophy response coincided with a reduction in serial sarcomere addition (Figure 5C; - 8.5%; p<0.001) compared to vehicle. Note that following 3-day UDD, rapamycin treated mice did not show significant increases in serial sarcomeres compared to untreated sham animals (Δ67 ± 81 sarcomeres, versus vehicle treated mice Δ363 ± 79 sarcomeres). This suggested rapamycin treatment almost completely inhibited longitudinal hypertrophy and that mTORC1

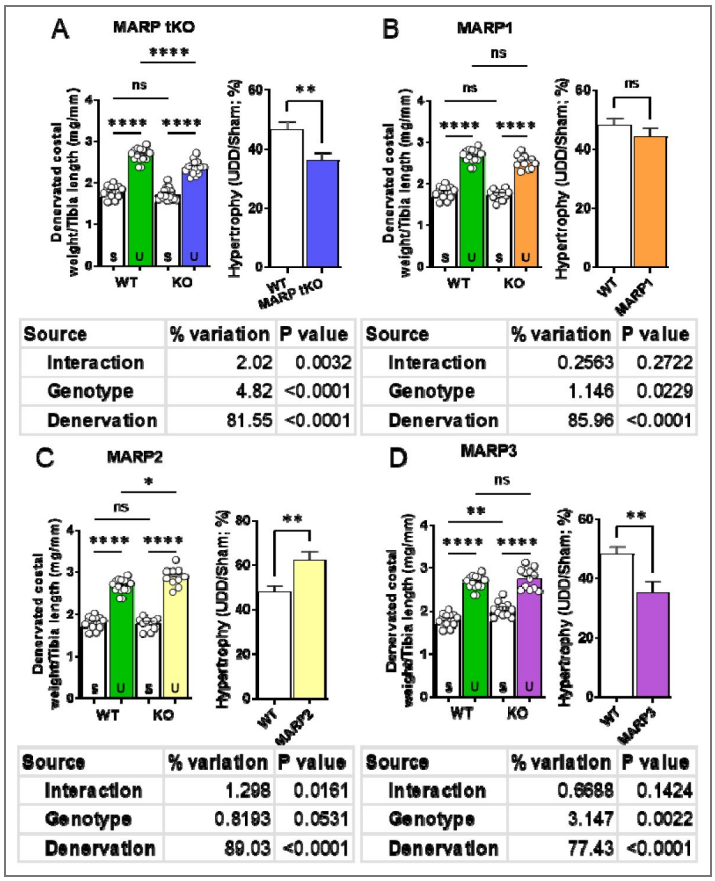

Source	% variation	P value
Interaction	2.02	0.0032
Genotype	4.82	<0.0001
Denervation	81.55	<0.0001

Source	% variation	P value
Interaction	0.2563	0.2722
Genotype	1.146	0.0229
Denervation	85.96	<0.0001

Source	% variation	P value
Interaction	1.298	0.0161
Genotype	0.8193	0.0531
Denervation	89.03	<0.0001

Source	% variation	P value
Interaction	0.6688	0.1424
Genotype	3.147	0.0022
Denervation	77.43	<0.0001

Figure 4. 6-day UDD on KO mice of MARP proteins.

MARP triple KOs show a reduced response to UDD (A; p<0.01). No effect of single MARP1 KO (B) on UDD, increased hypertrophy following MARP2 KO (B; p<0.01; t-test), indicating possible roles in hypertrophy suppression or atrophy signaling and MARP3 KO (C) showed baseline hypertrophy in costal diaphragm in addition to less hypertrophy development in UDD (p<0.01; t-test) compared to WT, implying roles as a suppressor of hypertrophy. Left panel, diaphragm right costal mass normalized to tibial length and right panel, percentual increase in right costal mass relative to sham. S= Sham, U= UDD (n=10-12). Statistical testing by t-test or two-way ANOVA with Tukey post-hoc testing.

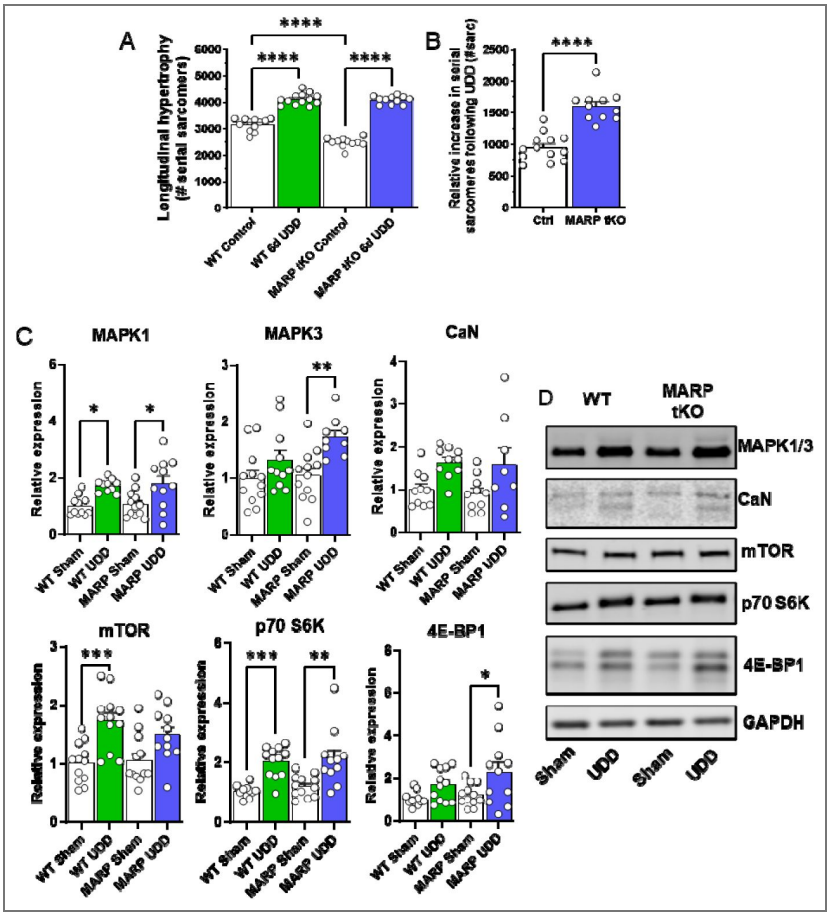

Figure 5. MARPs inhibits longitudinal hypertrophy.

Longitudinal hypertrophy measured in right costal strips of WT and MARP tKO mice in 6-day sham and UDD mice (A). Numerical increase in serial sarcomeres is higher in MARP tKO ($P<0.0001$) mice compared to WT mice (B; n=7-12), suggesting that the MARPs inhibits longitudinal growth. Probing hypertrophy signaling by western blot, normalized to Gapdh, with expression set relative to WT sham levels (C; n=8-12). Differential mTor response suggests role in regulating longitudinal hypertrophy. (D) Representative blot images of the signaling proteins. Statistical testing by one-way or two-way ANOVA with Tukey post-hoc testing.

signaling plays a vital role in longitudinal hypertrophy development. We thus propose that mTORC1 signaling positively regulates longitudinal hypertrophy in skeletal muscle and that titin's N2A-element tunes the extent of longitudinal hypertrophy through the MARPs to prevent excess hypertrophy (graphic summary in Figure 6G).

Discussion

Longitudinal hypertrophy as a mechanism for reducing stretch-induced mechanosensing

One of the most striking aspects of the UDD surgical model is the early transient hypertrophy. No other muscle denervation model induces hypertrophy, supporting the notion that stretch, even in inactive muscle, is a potent driver of hypertrophic growth. The extreme nature of the stretch at work in UDD, ~25% stretch of the denervated costal by the innervated costal at a frequency of 120-230 times a minute (respiration rate)[21], forms a potent trigger for muscle hypertrophy. Following 6-days UDD the denervated costal diaphragm develops 49.7±10.0% (Figure 1B) increase in mass, which is primarily caused by addition of 952±81 sarcomeres (Figure 1C) and to a lesser extent by radial fiber growth[21]. The transient nature of the hypertrophy can be explained by the reduction in sarcomere strain due to the addition of sarcomeres in series (longitudinal hypertrophy), removing the "trigger" that underlies the hypertrophy signaling. This hypothesis fits the data (Figure 1B-C), where before remodeling UDD costal width (i.e., fiber length) is ~8.7 mm (3000 sarcomeres x SL 2.9 µm), and when stretched 25%[21] equals a width of ~10.8 mm. Following 6-days hypertrophic remodeling (UDD), costal width is ~10.8 mm (4000 sarcomeres x SL 2.7 µm). This suggests that the costal width increase attenuates the hypertrophy trigger caused by stretching, finally resulting in atrophy (Figure 1B; 35-day UDD). Denervation itself does not appear to induce hypertrophy of the diaphragm, as 3-day BDD in rat showed no hypertrophy (Figure 1D-E). This does not exclude BDD-mediated denervation from potentially inhibiting or delaying the hypertrophy response. Denervated skeletal muscles have not been reported to experience (longitudinal) hypertrophy. UDD and BDD are both denervation models and hypertrophy occurs specifically in the denervated costal of UDD operated animals. Stretch is thus the mechanical difference between UDD and BDD and the trigger for hypertrophy signaling. BDD rats do experience abdominal breathing, which could stretch diaphragms sufficiently to induce longitudinal hypertrophy after an extended period of BDD. UDD being a denervation model shows that hypertrophy is not necessarily dependent on a muscle's ability to contract. This indicates that skeletal muscle may derive its signals for hypertrophy during the muscle relaxation-phase when the muscle is at its longest state. Muscle stretch in human is known to benefit muscle growth and is a vital part of exercise routines (reviewed in [24,25]). Perhaps muscle antagonism may provide sufficient stretch to induce hypertrophy. As contracting muscles inadvertently stretch their relaxed antagonists, they create an elegant feedback loop that promotes both muscle growth and the maintenance of muscle mass.

Titin's response to stretch

Titin's elastic properties have been extensively described[2,3]. These elastic properties are tied to titin's role in muscle trophicity, having a direct effect on the extent of muscle hypertrophy[20,21,26,27]. We showed that reducing titin stiffness, using both Rbm20 splice-deficient mice and rats, attenuated the stretch-based hypertrophy (Supplemental Figure 3). Importantly, in a model with increased titin stiffness, it was shown that titin stiffness has a direct effect on the number of sarcomeres in series[20], indicating that titin is a key regulator of longitudinal hypertrophy. Titin splicing analysis by RNA sequencing did not indicate changes in splicing in response to UDD (Supplemental Figure 2). Thus, stretch in rat diaphragm does not alter titin-based stiffness. In contrast, we observed reduced incorporation of exons encoding the PEVK

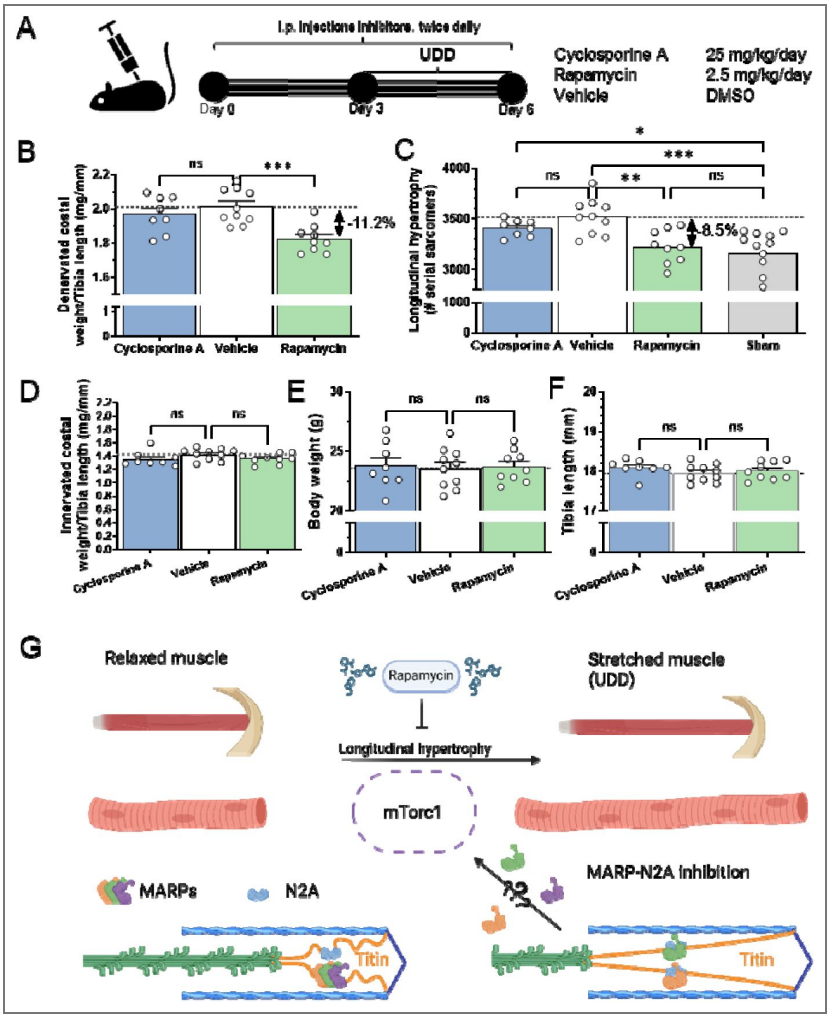

Figure 6. Pharmacological inhibition of the mTor (rapamycin) and calcium (cyclosporin A) based hypertrophy pathways revealed mTor to be involved in longitudinal hypertrophy.

(A) Schematic of the inhibition protocol, showing mice were injected with inhibitors for 3-days prior to receiving UDD surgery, with continued twice daily dosing of inhibitors until sacrifice at day 3 post-UDD. Rapamycin inhibited hypertrophy development both at the costal diaphragm mass level (B; $p<0.001$) and at the longitudinal hypertrophy level (C; $p<0.001$), whereas cyclosporine A had no effect. Neither cyclosporine A or rapamycin affected the innervated costal diaphragm (D), or body mass (E) and all mice used were of approximately the same size based on skeletal size, as measured by tibia length (F). (G) Hypothetical mechanism for longitudinal hypertrophy following muscle stretch. The mTorc1 pathway is activated by stretch and initiates longitudinal muscle hypertrophy. MARP proteins sequestered by titin's N2A element are released upon stretch and tunes the longitudinal hypertrophy, thus preventing excessive longitudinal hypertrophy (Image was generated using *BioRender.com*). N=8-10/group, statistical testing by 1-way-ANOVA and Dunnett's multiple comparisons test.

n in BDD rats which likely reflects inactivity promoting increased stiffness of titin. The exact mechanism underlying titin-based regulation of longitudinal hypertrophy is unclear and UDD does not alter titin-stiffness at the splicing level. Thus, we studied phosphorylation as a possible mechanism, focusing on signaling hot-spots in titin (reviewed in[5,22,28]) that could mediate longitudinal hypertrophy. Posttranslational changes in titin, particularly phosphorylation, have been studied mostly in relation to passive tension development[29–31]. Specific PTMs for titin have not been widely studied and only recently has ubiquitination been shown to recruit autophagic receptors to the kinase domain of titin[32,33]. Autophosphorylation of titin kinase at Y170 is considered one of the classic mechanosensing responses in titin resulting in phosphorylation of the autophagic receptor Nbr1 at S115/116, activating autophagy signaling in vitro[34]. We did not observe any signs following UDD that titin kinase was autophosphorylated at Y170. This could be related to phospho-peptide abundance being below the detection limit, or that the titin kinase is inactive[35]. In total we identified ~700 phosphorylation sites in titin of which 142 were significantly affected by stretch. These sites were distributed along the entire length of titin with several hot spots in the PEVK region, likely involved in stiffness regulation, and several in the Z-disk, which could be related to signaling or structural interactions. The sites in the N2A-element (Figure 3) were of particular interest as previously it has been suggested that S9540 (S9895 according to diaphragm RNAseq by Brynnel et al[20]) could serve as a recruitment signal for MARP1[36], a protein that is highly upregulated following UDD (Figure 2E). MARPs have been shown to quench N2A phosphorylation[36,37], which make the phosphorylation sites in the N2A segment tantalizing targets for studying titin-MARP binding. If S9459 and S9520 (Figure 3D-E) play such a role remains to be determined, but such insights could provide future avenues for manipulating titin-MARP interactions. Similarly, we found many titin-associated proteins to show differential phosphorylation in UDD, including 3 sites in the MARPs (Supplemental Figure 5). How these sites contribute to signaling or recruitment to the N2A-element remains to be seen but provide tantalizing targets for follow-up study.

The MARP proteins and muscle trophicity

Global transcriptome and proteome studies from 3-day UDD showed multiple titin-associated proteins being upregulated (Figure 2E). We focused our efforts on the MARP proteins, as they are known interacting partners of titin's N2A-element and have been shown to be important for hypertrophy regulation in the heart[38,39]. We used UDD on MARP KO mice, focusing on the triple KO for MARP1-3 to account for expected redundancy[7,37]. MARP tKO showed a 12% reduction in hypertrophy following 6-day UDD (Figure 4A). This suggested stretch-mechanosensing operated through the MARP proteins. In an attempt to isolate a single MARP protein as the main effector, we performed UDD on single MARP knock-out mice (Figure 4B-D). MARP1 KO did not reveal changes in hypertrophy. However, we previously established that MARP1 localizes to the N2A-segment of titin following UDD[21]. We also independently determined that MARP1 cross-links titin to the thin filament to increase passive tension[40,41], suggesting MARP1 plays mechanical roles over trophic regulation in skeletal muscle. MARP2 KO developed an exaggerated hypertrophy and lastly MARP3 KO showed an attenuated hypertrophy response to UDD, suggesting MARP2 and 3 play opposing roles in hypertrophy regulation. MARP2 interacts with Akt2[13], providing a tentative link with the mTOR pathway, discussed below. Additionally, MARP2 interaction with P50-NFκB acting as an analogue for IκB[14] suggests a possible role in inhibiting NFκB atrophy signaling. The role of MARP3 remains incompletely understood, but prior studies indicate that loss of MARP3 enhances glucose tolerance and insulin sensitivity[15], and MARP3 has been linked to AMPK signaling. AMPK is a key regulator of metabolic pathways and a well-established inhibitor of hypertrophic signaling, in part through suppression of mTOR activity, and is also responsive to mechanical stimuli [42,43]. To specifically determine if the MARPs affected longitudinal hypertrophy we measured the number of serial sarcomeres across the width of the costal diaphragm in MARP tKO and found that the tKO mice added 653.2 ± 91.55 more sarcomeres than WT following 6-day UDD (Figure 5B). This suggests that the MARP proteins inhibit longitudinal hypertrophy. A possible mechanism could be that following stretch the three MARPs bind and compete for the N2A-binding site[7,37] resulting in translocation of specific MARPs for signaling purposes. The benefit of

MARP deletion in cardiomyopathy was shown by Lange et al[10], where deletion of MARP1/2 ameliorated MLP KO induced DCM. MARP KO has not proven detrimental in mice[44], making this family an attractive target for therapeutic intervention.

mTOR and longitudinal hypertrophy

Muscle hypertrophy is regulated through a number of pathways, with the insulin-insulin growth factor (IGF) mediated pathway[45–47] being the most well understood in skeletal muscle and the calcineurin-NFAT pathway in cardiac muscle[48,49]. With most studies focused on radial (cross-sectional) hypertrophy, we aimed to gain insight into the regulatory mechanism underlying longitudinal hypertrophy, two types of hypertrophy that are not necessarily mutually exclusive. The mTOR signaling pathway was a prime candidate as UDD in MARP tKO mice suggested altered mTOR activity (Figure 5C-D). This prompted us to test inhibition of mTOR signaling and see if mTOR regulates longitudinal hypertrophy. Using rapamycin[50], an inhibitor that targets the mTORC1 (protein synthesis regulation) complex, we found a reduction in longitudinal hypertrophy following 3-days UDD compared to vehicle treated mice (Figure 6B). This strongly suggests that the mTORC1- pathway is in-part responsible for longitudinal hypertrophy following UDD. While rapamycin primarily inhibits mTORC1, rapamycin-insensitive signaling through mTORC2 may also contribute to UDD stretch-induced responses. Denervation itself may activate mTORC2-associated signaling pathways, which could confound the interpretation of stretch-specific versus denervation-mediated mTOR responses in this model. Therefore, a contribution of rapamycin-insensitive mTOR signaling to the observed phenotype cannot be excluded. Although we focused on mTOR signaling in longitudinal hypertrophy development, we do not exclude other pathways being important. mTOR formed an attractive target as previous work showed that longitudinal stretch phosphorylates Akt and upregulates MARP2[51], forming a tentative link between longitudinal stretch, MARPs and the mTOR pathway. mTORC1-based hypertrophy is primarily mediated through P70 S6K and 4E-BP1 and their respective phosphorylation signals at T389 and T37/46[46,47]. These sites were unchanged at 24-hour UDD (supplemental table 13) indicating that these sites are activated at a later stage, as reported by Norrby et al[52], or that mTOR is activated through alternative pathways following stretch. Further studies are needed to establish the roles of the various pathways in stretch hypertrophy.

In conclusion, we found that the transient hypertrophy induced by UDD is dependent on muscle fiber length, with longitudinal hypertrophy reducing the trigger for hypertrophy. The hypertrophy coincides with increased phosphorylation of the N2A element. The N2A-associated MARP proteins are strongly upregulated following UDD and deletion of the MARPs increases the extent of longitudinal hypertrophy following UDD, indicating the MARPs serve roles in inhibiting longitudinal hypertrophy. MARP tKO mice show altered regulation in the mTORC1 pathway following UDD and inhibition of mTORC1 by rapamycin shows mTOR is a main regulator of longitudinal hypertrophy.

Funding

This work was financially supported by National Institutes of Health grants R01HL121500 (CO), R01AR083233 (HG) and R35HL144998 (HG)

Methods

Animal studies

All experiments were done in accordance with the University of Arizona Institutional Animal Care and Use Committee and followed the US National Institutes of Health Using Animals in Intramural Research guidelines for animal use. We used 3-month-old C57BL/6J mice referred to as wildtype (WT), and 6-month-old Sprague Dawley rats (SD). Knockout models for titin binding proteins MARP1-3 (Ankrd1, Ankrd2 and Ankrd23)[10,44,53] were kindly provided by Dr Ju Chen and Dr

Stephan Lange. Homozygous Rbm20$^{\Delta RRM}$ mice [21,54] and Rbm20 ko rats[55,56], have previously been described. Mice were maintained on a C57BL/6J background, with the data from the MARP mice being on a black swiss background.

Surgical procedure

For unilateral diaphragm surgery (UDD)[21] or bilateral diaphragm denervation (BDD) studies, mice or rats were anaesthetized with 2-3% isoflurane and a small incision was made in the neck area just above the clavicle. The right phrenic nerve was isolated behind the sternohyoid muscle, and a 3–4 mm section was transected at the height of the supraclavicular nerve branch. For BDD surgery both left, and right phrenic nerves being transected. Sham operated animals underwent the same procedure, except the phrenic nerve was left intact. Animals were sacrificed 1, 3, 6, 12 or 35-days after surgery for morphometric analysis and tissue harvest.

Pharmacological inhibition of hypertrophy

Inhibitor studies with rapamycin (mTOR inhibitor) and cyclosporin A (Calcineurin inhibitor) were performed by injecting mice, twice daily intra-peritoneal (IP), with 2.5 or 25 mg/kg/day, respectively. Each inhibitor was dissolved in Dimethylsulfoxide (DMSO) and diluted to 20% DMSO with saline solution just before injection. Mice received inhibitors or vehicle (20% DMSO in saline) starting 3-days prior to UDD surgery to prime the mice and continued following UDD to inhibit hypertrophy growth (Figure 4C). Mice were sacrificed after 3-days UDD and processed for serial sarcomere measurements as described below.

Serial sarcomere measurements

Previously described in van der Pijl et al[21]. Briefly, mice were anaesthetized with a 140/10 mg/kg ketamine/xylazine solution, a small incision to visualize the jugular vein, which was subsequently cannulated for perfusion. Mice were perfused with a solution consisting of 4% formaldehyde, with 70 U/mL of heparin in phosphate buffered saline (PBS), after which the diaphragm was removed and stored in 4% formaldehyde in PBS overnight for complete fixation. Full length diaphragm midcostal strips were gently dissected and flattened between glass slides, costal width was measured using a caliper and sarcomere lengths were measured using a He/Ne laser diffraction system.

Alternatively, muscle fiber bundels from chemically demembranated full length diaphragm midcostal strips of 3-day mice were flattened between glass slides. Costal width and sarcomere lengths were measured using a Zeiss Axio Imager M1 microscope (Zeiss), at ×50 magnification to measure the length of the muscle bundles and ×640 for sarcomere length along four points of the fiber bundles. Images were captured using AxioCam MRc with Axiovision software (Zeiss) and images were calibrated using a 0.01 mm stage micrometre (Edmund Optics). To determine the number of serial sarcomeres the muscle bundle length (costal width) was divided by the sarcomere length.

Demembranating solution consisted of a relaxing solution (in mM; 20 BES, 10 EGTA, 6.56 MgCl2, 5.88 NaATP, 1 DTT, 46.35 K-propionate, 15 creatine phosphate, pH 7.0), with 1% Triton-X-100 at 4°C, and protease inhibitors (phenylmethylsulfonyl fluoride (PMSF), 0.25 mM; leupeptin, 0.04 mM; E64, 0.01 mM,), after demembranation, samples were stored in just relaxing solution plus inhibitors (without triton X-100) at 4°C.

Transcriptome studies

RNA sequencing (RNAseq) was performed on right costal diaphragm samples collected from 3-day sham and UDD animals and flash frozen in liquid nitrogen until further processing. For RNA extraction, samples were incubated overnight in RNAlater-ICE (Thermo Scientific) and subsequently transferred to RLT buffer for extraction according to the RNeasy Fibrous Tissue Mini Kit (Qiagen). Tissue disruption was achieved using a Bullet Blender (Next Advance) and Green Eppendorf lysis kit tubes (Next Advance), by grinding samples for 4 minutes at setting 10. Thereafter, total RNA extraction was performed following the RNeasy Fibrous Tissue Mini Kit's

instructions and quantified using a Nanodrop ND-1000 spectrophotometer (Thermo Scientific). Each sample consisted of 3 biological replicate sham or UDD samples. Both Library preparation and sequencing was performed by the University of Chicago Genomics Facility, Chicago, USA. Briefly, library preparation: rRNA was depleted from RNA preparations from 1 µg total RNA. Libraries were prepared using an RNA Library Prep Kit from Illumina following the manufacturer's instructions. Sequencing was performed on an Illumina Hiseq2500 sequencer using 100 bp paired-end sequencing. For RNAseq analysis see[20]. Briefly, Adapters and low-quality reads were removed with Trim Galore and reads were mapped to the rat genome (Release mRatBN7.2) using STAR[57] with default settings. Differentially expressed genes were determined with DESeq2[58]. Genes with population adjusted p-values (p_{adj}) <0.05 were considered differentially expressed. For titin splicing, percent spliced in index (PSI) was calculated as a measure for determining if an exon is spliced in, following the titin exon annotation by Bang et al.[59]. RNA sequence data were deposited at NIH NCBI BioProject (accession number PRJNA1460879).

Preparation of muscle for mass spectrometry analysis

Diaphragm muscle was ground to a fine powder using Dounce homogenizers cooled in liquid nitrogen and acclimated to –20°C for 30 min before continuing. Tissue powder was resuspended at a concentration of 50 mg/ml in a Urea buffer (4 M urea, 1 M thiourea, 25 mM Tris–HCl, 75 mM dithiothreitol, 1.5 % SDS, 25 % glycerol, pH 6.8) with protease inhibitors (0.04 mM E-64, 0.16 mM leupeptin, and 0.2 mM PMSF). The solution was mixed for 4 min, followed by 10 min of incubation at 60°C. Samples were centrifuged at 12.000 rpm and the supernatant flash frozen for storage at −80°C.

In-solution Tryptic Digestion

50 µg of rat costal diaphragm lysate was subjected to acetone precipitation by adding six times the sample volume of pre-chilled 100 % acetone and incubated one hour at -20°C. The precipitates were centrifuged at 16,000 x g for 10 minutes at 4°C and the acetone was removed.

400 µL of pre-chilled 90% acetone was added to the protein pellet, briefly vortexed and centrifuged at 16,000 x g for 5 minutes at 4°C. The remaining acetone was removed, the protein pellets were air dried for 3 minutes, resuspended in 100 µL of 50 mM NH_4HCO_3 and sonicated for 5 minutes. The samples were supplemented with dithiothreitol (DTT) at a final concentration of 5 mM and incubated at 70°C for 30 minutes. Samples were cooled to room temperature for 10 minutes and incubated with 15 mM acrylamide for 30 minutes at room temperature while protected from light. The reaction was quenched with DTT with a final concentration of 5 mM and incubated in the dark for 15 minutes. One µg of Lys-C was added to each sample and incubated at 37° C for 2-3 hours while shaking at 300 rpm followed by the addition of 50 µL of 50 mM ammonium bicarbonate and 2 µg of trypsin and incubation overnight at 37°C while shaking at 300 rpm. 14.7 µL of 40 % FA/1 % HFBA was added to each sample and incubated for 10 minutes (final concentration is 4 % FA/0.1 % HFBA) to stop trypsin digestion. The samples were desalted with Pierce Peptide Desalting Spin Columns per the manufacturer's protocol (ThermoFisher Scientific, cat no. 89852) and the peptides were dried by vacuum centrifugation. The dried peptides were resuspended in 20 µL of 0.1 % FA (v/v) and the peptide concentration was determined with the Pierce Quantitative Colorimetric Peptide Assay Kit per the manufacturer's protocol (ThermoFisher Scientific, cat no. 23275). 350 ng of the final sample was analyzed by mass spectrometry.

Phosphoproteomics

To determine global differences in protein phosphorylation abundance between sham or UDD, 1 mL of protein lysate corresponding to 50 mg diaphragm per sample (pooled costal diaphragm of 2 mice) was subjected to in-solution tryptic digestion and phosphopeptide enrichment using sequential enrichment from metal oxide affinity chromatography per manufacturer's protocol (Thermo Scientific, cat no. A32993 & A32992) similar to as previously described[60,61]. The dried

peptides were resuspended in 20 µL of 0.1 % FA (v/v) and the peptide concentration was determined with the Pierce Quantitative Colorimetric Peptide Assay Kit per the manufacturer's protocol. 350 ng of the final sample was then analyzed by mass spectrometry.

Mass Spectrometry

HPLC-ESI-MS/MS was performed in positive ion mode on a Thermo Scientific Orbitrap Fusion Lumos tribrid mass spectrometer fitted with an EASY-Spray Source (Thermo Scientific, San Jose, CA). NanoLC was performed using a Thermo Scientific UltiMate 3000 RSLCnano System with an EASY Spray C18 LC column (Thermo Scientific, 50cm x 75 µm inner diameter, packed with PepMap RSLC C18 material, 2 µm, cat. # ES803); loading phase for 15 min at 0.300 µL/min; mobile phase, linear gradient of 1–34 % Buffer B in 119 min at 0.220 JL /min, followed by a step to 95% Buffer B over 4 min at 0.220 µL/min, hold 5 min at 0.250 µL/min, and then a step to 1 % Buffer B over 5 min at 0.250 µL/min and a final hold for 10 min (total run 159 min); Buffer A = 0.1 % FA/H_2O; Buffer B = 0.1 % FA in 80 % ACN. All solvents were liquid chromatography mass spectrometry grade. Spectra were acquired using XCalibur, version 2.3 (ThermoFisher Scientific). A "TopSpeed" data-dependent MS/MS analysis was performed (acquisition of a full scan spectrum followed by collision-induced dissociation mass spectra of the Top N most intense precursor ions within the 3 second cycle time). Dynamic exclusion was enabled with a repeat count of 1, a repeat duration of 30 seconds, an exclusion list size of 500, and an exclusion duration of 40 seconds.

Label-free Quantitative Proteomics

Progenesis QI for proteomics software (version 2.4, Nonlinear Dynamics Ltd., Newcastle upon Tyne, UK) was used to perform ion-intensity based label-free quantification as previously described[62]. In brief, in an automated format, raw files were imported and converted into two-dimensional maps (y-axis = time, x-axis =m/z) followed by selection of a reference run for alignment purposes. An aggregate data set containing all peak information from all samples was created from the aligned runs, which was then further narrowed down by selecting only +2, +3, and +4 charged ions for further analysis. The samples were then grouped according to treatment. Peak lists of the top ten fragment ion spectra were exported in Mascot generic file (mgf) format and searched against either the 2020_06 Swiss-Prot *Rattus norvegicus* database (8128 entries) , the 2018_11 Swiss-Prot *Mus musculus* database (17008 entries), or species respective TrEMBL databases using Mascot (Matrix Science, London, UK; version 2.6.0). The search variables that were used were: 10 ppm mass tolerance for precursor ion masses and 0.5 Da for product ion masses; digestion with trypsin; a maximum of two missed tryptic cleavages; variable modifications of oxidation of methionine, phosphorylation of serine, threonine, and tyrosine, and carbamidomethylation of cysteine; 13C = 1. The resulting Mascot .xml file was then imported into Progenesis, allowing for peptide/protein assignment, while peptides with a Mascot Ion Score of <25 were not considered for further analysis. False discovery rate was set to 1% for both peptides (minimum length of 7 amino acids) and proteins. Abundances were normalized to the total ion current (TIC) to correct for differences in sample loading and instrument response. For quantification, proteins must have possessed at least one or more unique, identifying peptide.

Visualization and analysis of transcriptome and proteome data

Figures were generated using online resources, briefly, quantitative Venn diagrams were made using *https://www.biovenn.nl/*[63]. Lolipop graphs of gene onthology (GO) enritchment analysis by ShinyGO v0.75 *http://bioinformatics.sdstate.edu/go/*[64]. Heatmaps were generated using a combination of Graphpad Prism v9.1, Perseus v2.0.3.1[65] and Heatmapper (*http://heatmapper.ca/*)[66]. Perseus v2.0.3.1 was also used to analyze principal components and visualized using Graphpad Prism v9.1. A protein mapping table was constructed in R, using the R Interface to UniProt Web Services package version 2.34.0.[67] UniprotKB identifiers and gene ID's were assigned to each peptide. Phosphorylated peptides were mapped to the UniProt sequences to identify the positions of the modified residue(s) using stringr version 1.4.0.[68] For representation of titin phosphorylation, normalized abundance values were converted to Z-scores by subtracting the

grand-mean of normalized abundance values for a particular peptide and dividing by the grand-mean standard deviation. We subsequently summed Z-scores of isobaric peptides for a given phospho-site to generate values to represent expression levels. To generate domain or regional phosphorylation we further summed phospho-sites to derive domain and regional phosphorylation graphs.

Western blot

Western blot experiments previously described in van der Pijl et al[21]. Proteins were transferred onto Immobilon-P PVDF 0.45 µm membranes (Millipore) using semi dry transfer (Bio-Rad).

Membranes were blocked with Odyssey blocking buffer (Li-Cor Biosciences) for 1 hour, and subsequently probed with primary antibodies at 4°C overnight (See Table 1). Near Infra-Red dyes were used as secondary antibodies for detection with Odyssey CLx Imaging System (Li-Cor Biosciences, United states).

Antibody	Source/isotype	Dilution	Company	Catalog#
MAPK1/3 (ERK2/1)	Mouse IgG1	1:200	Cell Signaling	#4696
Calcineurin	Mouse IgG2a	1:750	BD biosciences	610260
mTOR	Rabbit IgG	1:750	Cell Signaling	#2983
P70S6K	Rabbit IgG	1:500	Cell Signaling	#2708
4EBP1	Rabbit IgG	1:750	Cell Signaling	#9452
Gapdh	Rabbit IgG	1:5000	Cell Signaling	#2112
Gapdh	Mouse IgG1	1:3000	Thermo Fisher Sci.	MA5-15738
CF790 Goat anti Mouse IgG	Goat IgG	1:10.000	Biotium	20342
CF680 Goat anti Mouse IgG	Goat IgG	1:10.000	Biotium	20065
CF680 Goat anti Rabbit IgG	Goat IgG	1:10.000	Biotium	20067
CF680R Goat anti Mouse IgG2a	Goat IgG	1:10.000	Biotium	20842

Table 1. Antibodies used in this study.

Supplementary figures

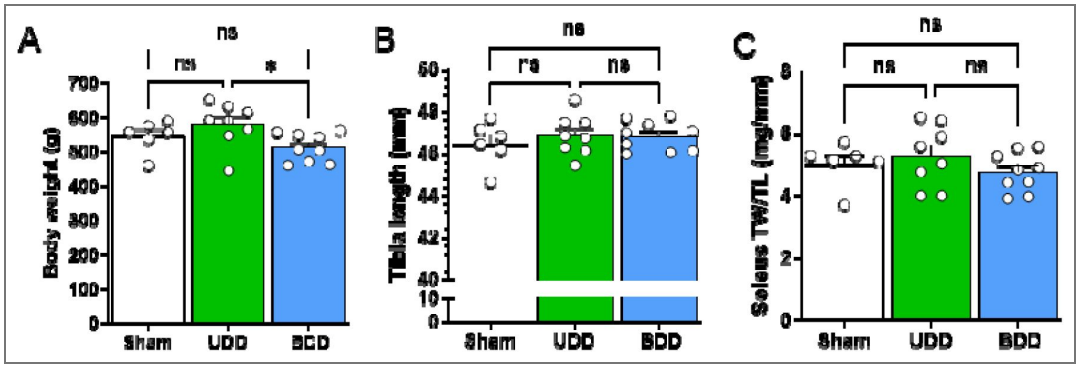

S Figure 1. 3-days bilateral diaphragm denervation in rats showed similar body weights compared to sham animals (A; n=6-9/group) and were of similar size based on tibia length (B) and soleus muscle weights (C). Statistical testing by one-way ANOVA and Dunnett's multiple comparisons test.

S Figure 2. Titin splicing in 3-day unilateral and bilateral diaphragm denervation in rats showed similar levels of splicing between UDD (red line) and sham (black line) animals, while BDD (blue line) animals showed a decrease in exons coding for the elastic PEVK element.

Statistical testing by Multiple t-testing, comparing sham to UDD and sham to BDD (n=4/group).

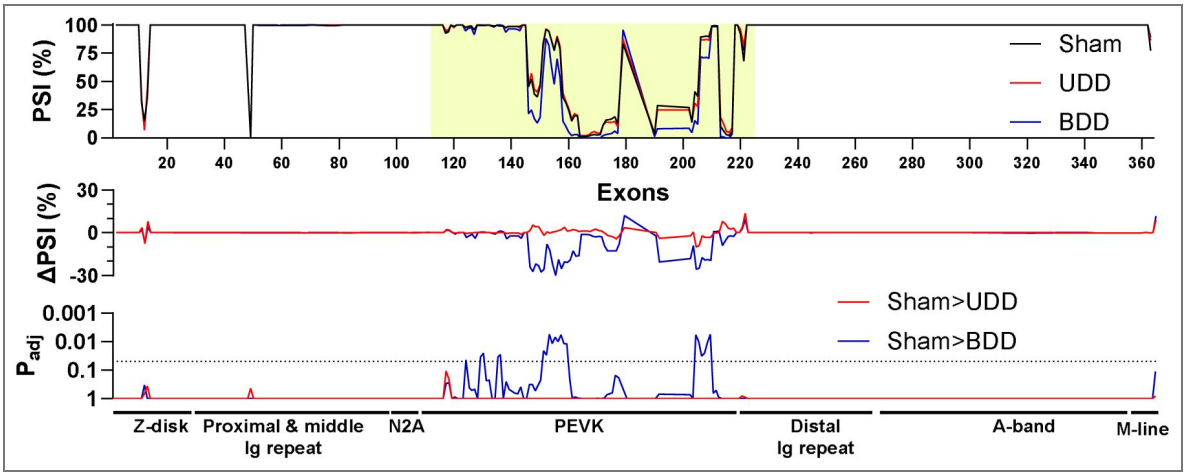

S Figure 3. Role of titin stiffness on hypertrophy following UDD.

(A) Transient hypertrophy response in Rbm20$^{\Delta RRM}$ mice (more compliant titin) showing a blunted hypertrophy response compared to WT mice, based on percent increase of diaphragm right costal mass relative to sham (n=10-12). (B) Titin-based stiffness does not alter longitudinal hypertrophy response, as both WT and Rbm20$^{\Delta RRM}$ mice show a similar increase in serial sarcomeres following 6-days UDD. Rbm20-KO rat response to 3-days UDD, based on percent increase of diaphragm right costal mass relative to sham (mouse n=10-11, rat n=8) supporting titin-based stiffness regulating muscle hypertrophy similarly across species. Statistical testing by t-test.

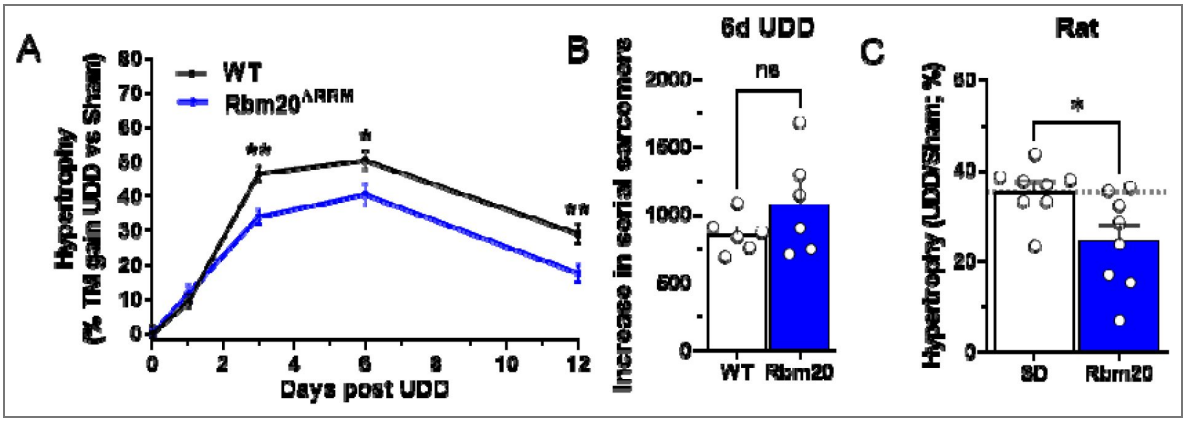

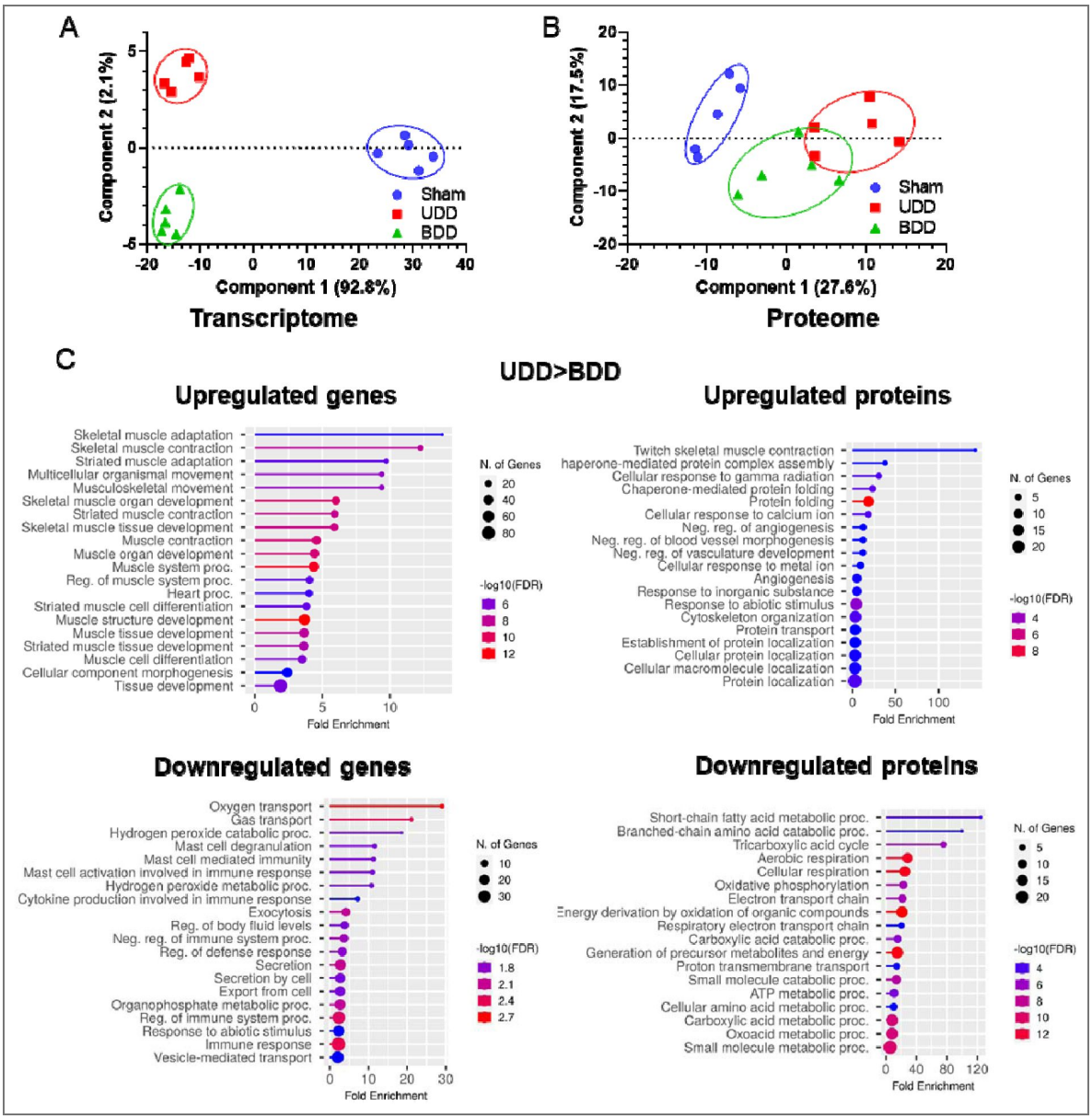

S Figure 4. Principal component analysis of the rat 3-day UDD and BDD transcriptome (A) and proteome (B), showing clear separation of groups at the transcript level and overlap of BDD and UDD samples at the protein level.

GOterm enrichment of UDD>BDD separated by up- or down-regulated transcriptomes and proteome (C, left and right, respectively) show distinct, yet overlapping cellular processes. Global mass spectrometry was analyzed by ANOVA and corrected for multiple comparisons with false discovery rate with a cut-off at p<0.05.

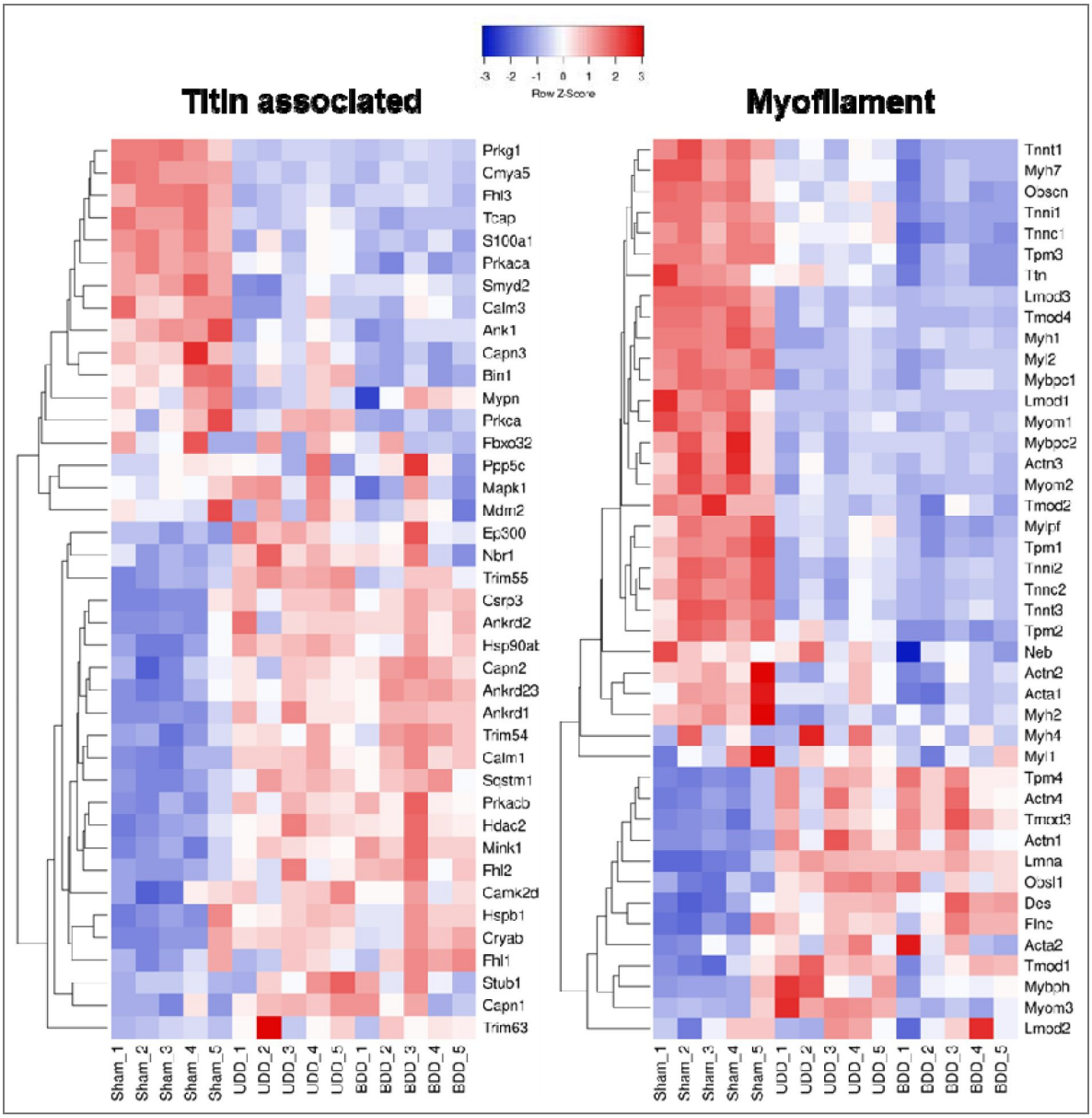

S Figure 5. Transcriptome regulation of titin-associated and myofilament genes by RNAseq in rats following 3-days of UDD/BDD.

Heatmaps showing similar regulation between UDD and BDD samples (n=4-5; Z-score: red= upregulated, blue= downregulated) at the transcript level for titin-associated and myofilament genes, based on hierarchal clustering.

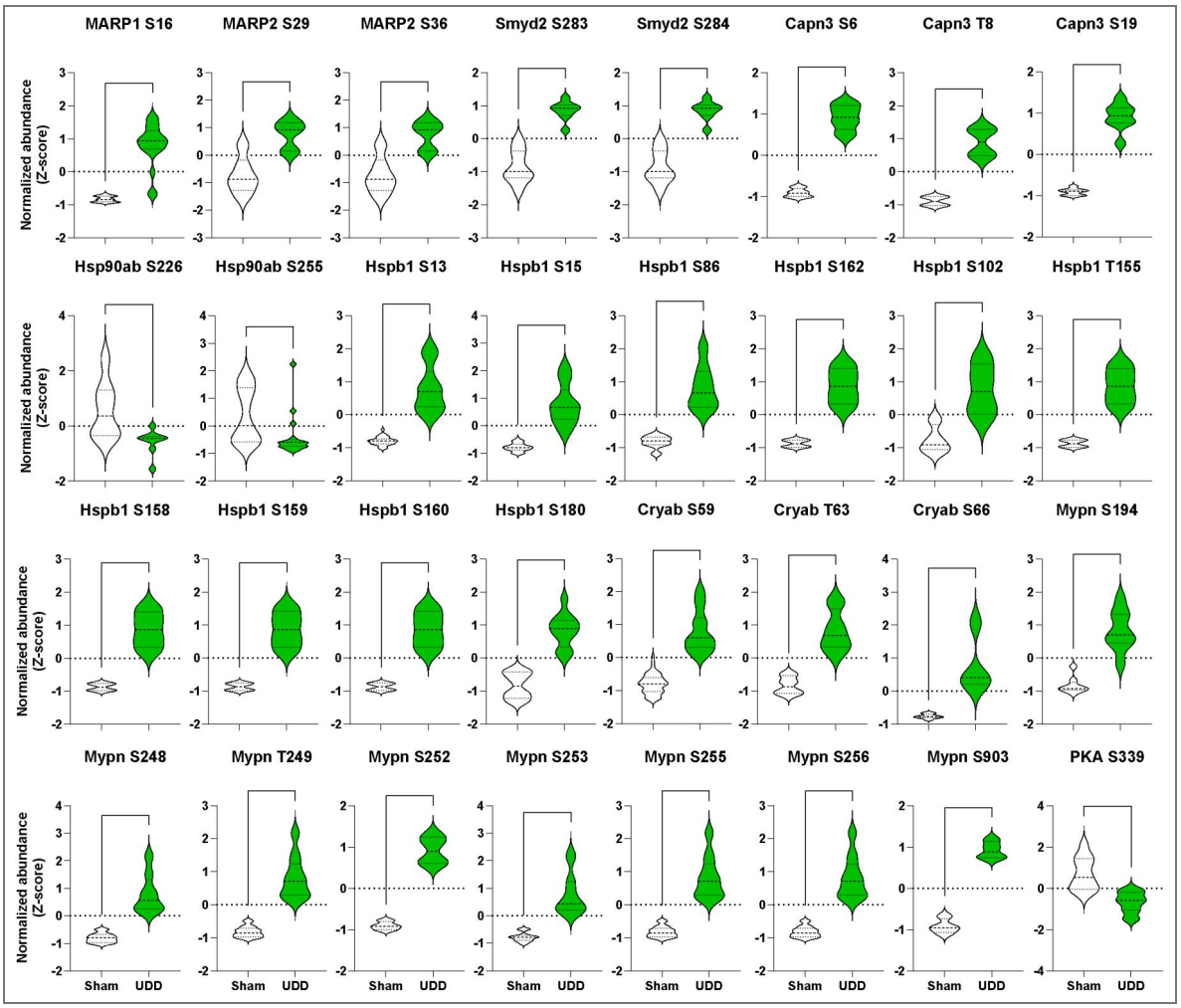

S Figure 6. Titin N2A associated protein phosphorylation events at 24-hour UDD.

Violin plots of phosphorylation events in N2A-associated proteins following UDD: MARP1 (Transcript: ENSMUST00000237142.2 Ankrd1-205), MARP2 (Transcript: ENSMUST00000026172.3 Ankrd2-201), Smyd2 (Transcript: ENSMUST00000027897.8 Smyd2-201), Capn3 (Transcript: ENSMUST00000028749.15 Capn3-202), Hsp90ab (Transcript: ENSMUST00000024739.14 Hsp90ab1-201), Mypn (Transcript: ENSMUST00000095580.3 Mypn-201), Hspb1 (Transcript: ENSMUST00000005077.7 Hspb1-201), Cryab (Transcript: ENSMUST00000217475.2 Cryab-206) and Prkca/PKA (Transcript: ENSMUST00000005606.8 Prkaca-201). Data represented as Log2 of the normalized abundance with significance determined by Kolmogorov-Smirnov test.

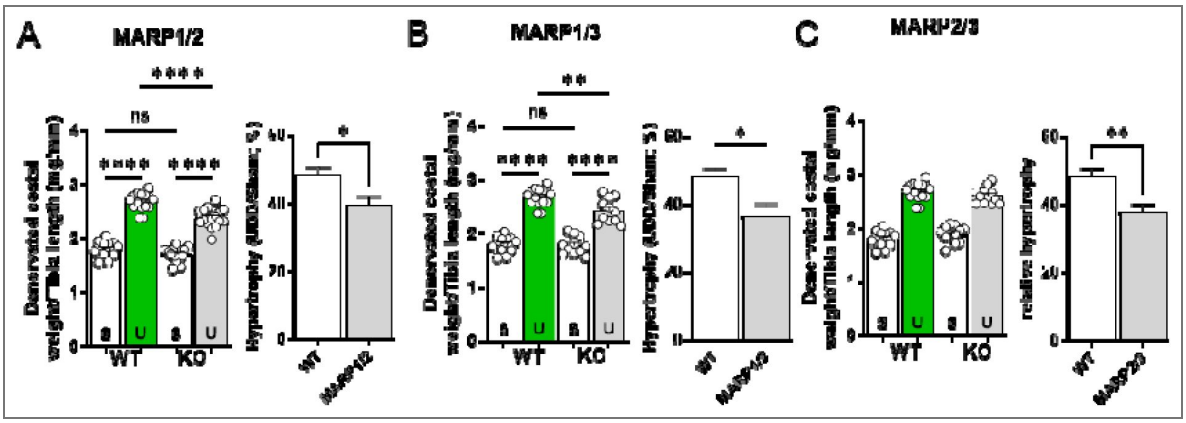

S Figure 7. **6-day UDD on double KO mice of MARPs.**

Double KO of MARP1/2 (A), MARP1/3 (B) and MARP2/3 (C) all showed a reduction in hypertrophy following UDD, suggesting redundancy between the MARPs. Left panel, diaphragm right costal mass normalized to tibial length and right panel, percentual increase in right costal mass relative to sham. S= Sham, U= UDD (n=10-12).

Data availability

NA sequence data were deposited in BioProject (accession number PRJNA1460879). All data generated or analyzed during this study are included in the manuscript and supporting files

Additional files

Supplemental tables.

Additional information

Funding

Funder	Grant reference number	Author
HHS | NIH | National Heart, Lung, and Blood Institute (NHLBI)	R01HL121500	Coen Ottenheijm
HHS | NIH | National Institute of Arthritis and Musculoskeletal and Skin Diseases (NIAMS)	R01AR083233	Henk L Granzier
HHS | NIH | National Heart, Lung, and Blood Institute (NHLBI)	R35HL144998	Henk L Granzier
American Heart Association (AHA)	2021AHA000POST000215904	Robbert van der Pijl

Author ORCID iDs

Henk Granzier: https://orcid.org/0000-0002-9516-407X

References

1. **Labeit S,** Kolmerer B (1995) Titins: giant proteins in charge of muscle ultrastructure and elasticity. *Science* **270**:293-296 https://doi.org/10.1126/science.270.5234.293 | PubMed
2. **Horowits R,** Kempner ES, Bisher ME, Podolsky RJ (1986) A physiological role for titin and nebulin in skeletal muscle. *Nature* **323**:160-164 https://doi.org/10.1038/323160a0 | PubMed
3. **Swist S,** Unger A, Li Y, et al. (2020) Maintenance of sarcomeric integrity in adult muscle cells crucially depends on Z-disc anchored titin. *Nat Commun* **11**:4479 https://doi.org/10.1038/s41467-020-18131-2 | PubMed
4. **Ottenheijm CAC,** van Hees HWH, Heunks LMA, Granzier H (2011) Titin-based mechanosensing and signaling: role in diaphragm atrophy during unloading?. *Am J Physiol Lung Cell Mol Physiol* **300**:L161-6 https://doi.org/10.1152/ajplung.00288.2010 | PubMed
5. **van der Pijl RJ,** Granzier HL, Ottenheijm CAC (2019) Diaphragm contractile weakness due to reduced mechanical loading: role of titin. *Am J Physiol Cell Physiol* **317**:C167-C176 https://doi.org/10.1152/ajpcell.00509.2018 | PubMed
6. **Voelkel T,** Linke WA (2011) Conformation-regulated mechanosensory control via titin domains in cardiac muscle. *Pflugers Arch* **462**:143-154 https://doi.org/10.1007/s00424-011-0938-1 | PubMed
7. **Miller MK,** Bang ML, Witt CC, et al. (2003) The muscle ankyrin repeat proteins: CARP, ankrd2/Arpp and DARP as a family of titin filament-based stress response molecules. *J Mol Biol.* **333**:951-964 https://doi.org/10.1016/j.jmb.2003.09.012 | PubMed
8. **Wette SG,** Smith HK, Lamb GD, Murphy RM (2017) Characterization of muscle ankyrin repeat proteins in human skeletal muscle. *Am J Physiol Cell Physiol* **313**:C327-C339 https://doi.org/10.1152/ajpcell.00077.2017 | PubMed
9. **Hayashi C,** Ono Y, Doi N, et al. (2008) Multiple molecular interactions implicate the connectin/titin N2A region as a modulating scaffold for p94/calpain 3 activity in skeletal muscle. *Journal of Biological Chemistry* **283**:14801-14814 https://doi.org/10.1074/jbc.M708262200 | PubMed

10. **Lange S,** Gehmlich K, Lun AS, et al. (2016) MLP and CARP are linked to chronic PKCalpha signalling in dilated cardiomyopathy. *Nat Commun* **7**:12120 https://doi.org/10.1038/ncomms12120 | PubMed
11. **van der Pijl RJ,** van den Berg M, van de Locht M, et al. (2021) Muscle ankyrin repeat protein 1 (MARP1) locks titin to the sarcomeric thin filament and is a passive force regulator. *Journal of General Physiology* **153** https://doi.org/10.1085/jgp.202112925 | PubMed
12. **Zhou T,** Fleming JR, Lange S, et al. (2021) Molecular Characterisation of Titin N2A and Its Binding of CARP Reveals a Titin/Actin Cross-linking Mechanism. *J Mol Biol* **433** https://doi.org/10.1016/j.jmb.2021.166901 | PubMed
13. **Cenni V,** Bavelloni A, Beretti F, et al. (2011) Ankrd2/ARPP is a novel Akt2 specific substrate and regulates myogenic differentiation upon cellular exposure to H(2)O(2). *Mol Biol Cell* **22**:2946-2956 https://doi.org/10.1091/mbc.E10-11-0928 | PubMed
14. **Bean C,** Verma NK, Yamamoto DL, et al. (2014) Ankrd2 is a modulator of NF-κB-mediated inflammatory responses during muscle differentiation. *Cell Death Dis* **5**:e1002 https://doi.org/10.1038/cddis.2013.525 | PubMed
15. **Shimoda Y,** Matsuo K, Kitamura Y, et al. (2015) Diabetes-Related Ankyrin Repeat Protein (DARP/Ankrd23) Modifies Glucose Homeostasis by Modulating AMPK Activity in Skeletal Muscle. *PLoS One* **10**:e0138624 https://doi.org/10.1371/journal.pone.0138624 | PubMed
16. **Laughlin MH,** Yang HT, Tharp DL, Rector RS, Padilla J, Bowles DK (2017) Vascular cell transcriptomic changes to exercise training differ directionally along and between skeletal muscle arteriolar trees. *Microcirculation* **24** https://doi.org/10.1111/micc.12336 | PubMed
17. **Mayans O,** van der Ven PF, Wilm M, et al. (1998) Structural basis for activation of the titin kinase domain during myofibrillogenesis. *Nature* **395**:863-869 https://doi.org/10.1038/27603 | PubMed
18. **Bertz M,** Wilmanns M, Rief M (2009) The titin-telethonin complex is a directed, superstable molecular bond in the muscle Z-disk. *Proc Natl Acad Sci U S A* **106**:13307-133310 https://doi.org/10.1073/pnas.0902312106 | PubMed
19. **van der Pijl RJ,** Hudson B, Granzier-Nakajima T, et al. (2020) Deleting Titin's C-Terminal PEVK Exons Increases Passive Stiffness, Alters Splicing, and Induces Cross-Sectional and Longitudinal Hypertrophy in Skeletal Muscle. *Front Physiol* **11**:494 https://doi.org/10.3389/fphys.2020.00494 | PubMed
20. **Brynnel A,** Hernandez Y, Kiss B, et al. (2018) Downsizing the molecular spring of the giant protein titin reveals that skeletal muscle titin determines passive stiffness and drives longitudinal hypertrophy. *eLife* **7**:e40532 https://doi.org/10.7554/eLife.40532 | PubMed
21. **van der Pijl R,** Strom J, Conijn S, et al. (2018) Titin-based mechanosensing modulates muscle hypertrophy. *J Cachexia Sarcopenia Muscle* **9**:947-961 https://doi.org/10.1002/jcsm.12319 | PubMed
22. **van der Pijl RJ,** Domenighetti AA, Sheikh F, Ehler E, Ottenheijm CAC, Lange S (2021) The titin N2B and N2A regions: biomechanical and metabolic signaling hubs in cross-striated muscles. *Biophys Rev* **13**:653-677 https://doi.org/10.1007/s12551-021-00836-3 | PubMed
23. **Bang ML,** Centner T, Fornoff F, et al. (2001) The complete gene sequence of titin, expression of an unusual approximately 700-kDa titin isoform, and its interaction with obscurin identify a novel Z-line to I-band linking system. *Circ Res* **89**:1065-1072 https://doi.org/10.1161/hh2301.100981 | PubMed
24. **Nunes JP,** Schoenfeld BJ, Nakamura M, Ribeiro AS, Cunha PM, Cyrino ES (2020) Does stretch training induce muscle hypertrophy in humans? A review of the literature. *Clin Physiol Funct Imaging* **40**:148-156 https://doi.org/10.1111/cpf.12622 | PubMed
25. **Warneke K,** Lohmann LH, Lima CD, et al. (2023) Physiology of Stretch-Mediated Hypertrophy and Strength Increases: A Narrative Review. *Sports Medicine* **53**:2055-2075 https://doi.org/10.1007/s40279-023-01898-x | PubMed
26. **Strom J,** Bull M, Gohlke J, et al. (2024) Titin's cardiac-specific N2B element is critical to mechanotransduction during volume overload of the heart. *J Mol Cell Cardiol* **191**:40-49 https://doi.org/10.1016/j.yjmcc.2024.04.006 | PubMed

27. **Methawasin M,** Strom JG, Slater RE, Fernandez V, Saripalli C, Granzier HL (2016) Experimentally Increasing Titin's Compliance Through RBM20 Inhibition Improves Diastolic Function in a Mouse Model of HFpEF. *Circulation* **20**:CIRCULATIONAHA.116.023003 https://doi.org/10.1161/CIRCULATIONAHA.116.023003 | PubMed

28. **Voelkel T,** Linke W a. (2011) Conformation-regulated mechanosensory control via titin domains in cardiac muscle. *Pflugers Arch* **462**:143-154 https://doi.org/10.1007/s00424-011-0938-1 | PubMed

29. **Hidalgo C,** Granzier H (2013) Tuning the molecular giant titin through phosphorylation: Role in health and disease. *Trends Cardiovasc Med* **23**:165-171 https://doi.org/10.1016/j.tcm.2012.10.005 | PubMed

30. **Krüger M,** Kötter S, Grützner A, et al. (2009) Protein kinase G modulates human myocardial passive stiffness by phosphorylation of the titin springs. *Circ Res* **104**:87-94 https://doi.org/10.1161/CIRCRESAHA.108.184408 | PubMed

31. **Loescher CM,** Hobbach AJ, Linke WA (2022) Titin (TTN): from molecule to modifications, mechanics, and medical significance. *Cardiovasc Res* **118** https://doi.org/10.1093/cvr/cvab328 | PubMed

32. **Müller E,** Salcan S, Bongardt S, Barbosa DM, Krüger M, Kötter S (2021) E3-ligase knock down revealed differential titin degradation by autophagy and the ubiquitin proteasome system. *Sci Rep* **11** https://doi.org/10.1038/s41598-021-00618-7 | PubMed

33. **Bogomolovas J,** Fleming JR, Franke B, et al. (2021) Titin kinase ubiquitination aligns autophagy receptors with mechanical signals in the sarcomere. *EMBO Rep* **22** https://doi.org/10.15252/embr.201948018 | PubMed

34. **Lange S,** Xiang F, Yakovenko a, et al. (2005) The kinase domain of titin controls muscle gene expression and protein turnover. *Science ...* **308**:1599-1603 https://doi.org/10.1126/science.1110463 | PubMed

35. **Bogomolovas J,** Gasch A, Simkovic F, Rigden DJ, Labeit S, Mayans O (2014) Titin kinase is an inactive pseudokinase scaffold that supports MuRF1 recruitment to the sarcomeric M-line. *Open Biol* **4**:140041 https://doi.org/10.1098/rsob.140041 | PubMed

36. **Lanzicher T,** Zhou T, Saripalli C, et al. (2020) Single-Molecule Force Spectroscopy on the N2A Element of Titin: Effects of Phosphorylation and CARP. *Front Physiol* **11**:173 https://doi.org/10.3389/fphys.2020.00173 | PubMed

37. **Lun AS,** Chen J, Lange S (2014) Probing Muscle Ankyrin-Repeat Protein (MARP) structure and function. *Anatomical Record* **297**:1615-1629 https://doi.org/10.1002/ar.22968 | PubMed

38. **Zhong L,** Chiusa M, Cadar AG, et al. (2015) Targeted inhibition of ANKRD1 disrupts sarcomeric ERK-GATA4 signal transduction and abrogates phenylephrine-induced cardiomyocyte hypertrophy. *Cardiovasc Res* **106**:261-271 https://doi.org/10.1093/cvr/cvv108 | PubMed

39. **Lange S,** Gehmlich K, Lun AS, et al. (2016) MLP and CARP are linked to chronic PKCα signalling in dilated cardiomyopathy. *Nat Commun* **7**:12120 https://doi.org/10.1038/ncomms12120 | PubMed

40. **van der Pijl RJ,** van den Berg M, van de Locht M, et al. (2021) Muscle ankyrin repeat protein 1 (MARP1) locks titin to the sarcomeric thin filament and is a passive force regulator. *Journal of General Physiology* **153** https://doi.org/10.1085/jgp.202112925 | PubMed

41. **Zhou T,** Fleming JR, Lange S, et al. (2021) Molecular Characterisation of Titin N2A and Its Binding of CARP Reveals a Titin/Actin Cross-linking Mechanism. *J Mol Biol* **433** https://doi.org/10.1016/j.jmb.2021.166901 | PubMed

42. **Budinger GRS,** Urich D, DeBiase PJ, et al. (2008) Stretch-induced activation of AMP kinase in the lung requires dystroglycan. *Am J Respir Cell Mol Biol* **39**:666-672 https://doi.org/10.1165/rcmb.2007-0432OC | PubMed

43. **Shimoda Y,** Matsuo K, Kitamura Y, et al. (2015) Diabetes-Related Ankyrin Repeat Protein (DARP/Ankrd23) Modifies Glucose Homeostasis by Modulating AMPK Activity in Skeletal Muscle. *PLoS One* **10**:e0138624 https://doi.org/10.1371/journal.pone.0138624 | PubMed

44. **Barash IA,** Bang ML, Mathew L, Greaser ML, Chen J, Lieber RL (2007) Structural and regulatory roles of muscle ankyrin repeat protein family in skeletal muscle. *Am J Physiol Cell Physiol* **293**:C218-C227 https://doi.org/10.1152/ajpcell.00055.2007 | PubMed

45. **Schiaffino S,** Mammucari C (2011) Regulation of skeletal muscle growth by the IGF1-Akt/PKB pathway: insights from genetic models. *Skelet Muscle* **1**:4 https://doi.org/10.1186/2044-5040-1-4 | PubMed

46. **Goodman CA** (2019) Role of mTORC1 in mechanically induced increases in translation and skeletal muscle mass. *J Appl Physiol (1985)* **127**:581-590 https://doi.org/10.1152/japplphysiol.01011.2018 | PubMed

47. **Yoon MS** (2017) mTOR as a Key Regulator in Maintaining Skeletal Muscle Mass. *Front Physiol* **8**:788 https://doi.org/10.3389/fphys.2017.00788 | PubMed

48. **Molkentin JD** (2004) Calcineurin-NFAT signaling regulates the cardiac hypertrophic response in coordination with the MAPKs. *Cardiovasc Res* **63**:467-475 https://doi.org/10.1016/j.cardiores.2004.01.021 | PubMed

49. **Molkentin JD** (2013) Parsing good versus bad signaling pathways in the heart: role of calcineurin-nuclear factor of activated T-cells. *Circ Res* **113**:16-19 https://doi.org/10.1161/CIRCRESAHA.113.301667 | PubMed

50. **Li J,** Kim SG, Blenis J (2014) Rapamycin: one drug, many effects. *Cell Metab* **19**:373-379 https://doi.org/10.1016/j.cmet.2014.01.001 | PubMed

51. **Mohamed JS,** Lopez MA, Cox GA, Boriek AM (2010) Anisotropic regulation of Ankrd2 gene expression in skeletal muscle by mechanical stretch. *The FASEB Journal* **24**:3330-3340 https://doi.org/10.1096/fj.10-158386 | PubMed

52. **Norrby M,** Evertsson K, Fjallstrom AK, Svensson A, Tagerud S (2012) Akt (protein kinase B) isoform phosphorylation and signaling downstream of mTOR (mammalian target of rapamycin) in denervated atrophic and hypertrophic mouse skeletal muscle. *J Mol Signal* **7**:7 https://doi.org/10.1186/1750-2187-7-7 | PubMed

53. **Bang ML,** Gu Y, Dalton ND, Peterson KL, Chien KR, Chen J (2014) The muscle ankyrin repeat proteins CARP, Ankrd2, and DARP are not essential for normal cardiac development and function at basal conditions and in response to pressure overload. *PLoS One.* **9**:e93638 https://doi.org/10.1371/journal.pone.0093638 | PubMed

54. **Methawasin M,** Hutchinson KR, Lee EJ, et al. (2014) Experimentally increasing titin compliance in a novel mouse model attenuates the Frank-Starling mechanism but has a beneficial effect on diastole. *Circulation* **129**:1924-1936 https://doi.org/10.1161/CIRCULATIONAHA.113.005610 | PubMed

55. **Li S,** Guo W, Dewey CN, Greaser ML (2013) Rbm20 regulates titin alternative splicing as a splicing repressor. *Nucleic Acids Res* **41**:2659-2672 https://doi.org/10.1093/nar/gks1362 | PubMed

56. **Lindqvist J,** van den Berg M, van der Pijl R, et al. (2018) Positive End-Expiratory Pressure Ventilation Induces Longitudinal Atrophy in Diaphragm Fibers. *Am J Respir Crit Care Med* **198**:472-485 https://doi.org/10.1164/rccm.201709-1917OC | PubMed

57. **Dobin A,** Davis CA, Schlesinger F, et al. (2013) STAR: ultrafast universal RNA-seq aligner. *Bioinformatics* **29**:15-21 https://doi.org/10.1093/bioinformatics/bts635 | PubMed

58. **Love MI,** Huber W, Anders S (2014) Moderated estimation of fold change and dispersion for RNA-seq data with DESeq2. *Genome Biol* **15**:550 https://doi.org/10.1186/s13059-014-0550-8 | PubMed

59. **Bang ML,** Centner T, Fornoff F, et al. (2001) The Complete Gene Sequence of Titin, Expression of an Unusual 700-kDa Titin Isoform, and Its Interaction With Obscurin Identify a Novel Z-Line to I-Band Linking System. *Circ Res.* **89**:1065-1072 https://doi.org/10.1161/hh2301.100981 | PubMed

60. **Levine AA,** Liktor-Busa E, Balasubramanian S, et al. (2023) Depletion of Endothelial-Derived 2-AG Reduces Blood-Endothelial Barrier Integrity via Alteration of VE-Cadherin and the Phospho-Proteome. *Int J Mol Sci* **25**:531 https://doi.org/10.3390/ijms25010531 | PubMed

61. **Keresztes A,** Olson K, Nguyen P, et al. (2022) Antagonism of the mu-delta opioid receptor heterodimer enhances opioid antinociception by activating Src and calcium/calmodulin-dependent protein kinase II signaling. *Pain* **163**:146-158 https://doi.org/10.1097/j.pain.0000000000002320 | PubMed

62. **Parker SS,** Krantz J, Kwak EA, et al. (2019) Insulin Induces Microtubule Stabilization and Regulates the Microtubule Plus-end Tracking Protein Network in Adipocytes. *Mol Cell Proteomics* **18**:1363-1381 https://doi.org/10.1074/mcp.RA119.001450 | PubMed

63. **Hulsen T,** de Vlieg J, Alkema W (2008) BioVenn – a web application for the comparison and visualization of biological lists using area-proportional Venn diagrams. *BMC Genomics* **9** https://doi.org/10.1186/1471-2164-9-488 | PubMed

64. **Ge SX,** Jung D, Yao R (2020) ShinyGO: a graphical gene-set enrichment tool for animals and plants. *Bioinformatics* **36** https://doi.org/10.1093/bioinformatics/btz931 | PubMed

65. **Tyanova S,** Temu T, Sinitcyn P, et al. (2016) The Perseus computational platform for comprehensive analysis of (prote)omics data. *Nat Methods* **13** https://doi.org/10.1038/nmeth.3901 | PubMed

66. **Babicki S,** Arndt D, Marcu A, et al. (2016) Heatmapper: web-enabled heat mapping for all. *Nucleic Acids Res* **44** https://doi.org/10.1093/nar/gkw419 | PubMed

67. **Carlson M,** Ortutay C, Ramos M (2021) R Interface to UniProt Web Services. Bioconductor.. version: 2.34.0 https://doi.org/10.18129/B9.bioc.UniProt.ws

68. **Wickham H.** (2019) stringr: Simple, Consistent Wrappers for Common String Operations. Github. version: 1.4.0 https://doi.org/10.32614/CRAN.package.stringr

van der Pijl R, Gohlke J, Strom J, Peters E, Shen S, Conijn S, Hourani Z, Lange S, Chen J, Langlais P, *et al.* (2026) The titin N2A-MARP signalosome constrains muscle longitudinal hypertrophy in response to stretch. NCBI BioProject. ID PRJNA1460879 https://www.ncbi.nlm.nih.gov/bioproject/?term=PRJNA1460879

Peer reviews

Reviewer #1 (Public review):

[Editors' note: this version has been assessed by the Reviewing Editor without further input from the original reviewers. The authors have addressed the comments raised in the previous round of review.]

Summary:

In this manuscript, the authors employ diaphragm denervation in rats and mice to study titin-based mechanosensing and longitudinal muscle hypertrophy. By integrating bulk RNA-seq, proteomics, and phosphoproteomics, they map the stretch-responsive signalling landscape, uncovering robust induction of the muscle-ankyrin-repeat proteins (MARP1-3) together with enhanced phosphorylation of titin's N2A element.

Genetic ablation of MARPs in mice amplifies longitudinal fibre growth and is accompanied by activation of the mTOR pathway, whereas systemic rapamycin treatment suppresses the hypertrophic response, highlighting mTORC1 as a key downstream effector of titin/MARP signalling.

Strengths:

The authors address a clear biological question: "how titin-associated factors translate mechanical stretch into longitudinal fibre growth" using a unique and clinically relevant animal model of diaphragm denervation. Using a comprehensive multiomics approach, the authors identify MARPs as potential mediators of these effects and use a genetic mouse model to provide compelling evidence supporting causality. Additionally, connecting these findings

to rapamycin, a drug widely used clinically, further increases the relevance and potential impact of the study.

https://doi.org/10.7554/eLife.107597.2.sa2

Reviewer #2 (Public review):

Summary:

Muscle hypertrophy is a major regulator of human health and performance. Here, van der Pilj and colleagues assess the role of the giant elastic protein, titin, in regulating the longitudinal hypertrophy of diaphragm muscles following denervation. Interestingly, the authors find an early hypertrophic response, with 30% new serial sarcomeres added within 6 days, followed by subsequent muscle atrophy. Using RBM20 mutant mice, which express a more compliant titin, the authors discovered that this longitudinal hypertrophy is mediated via titin mechanosensing. Through an omics approach, it is suggested that the Muscle ankyrin proteins may regulate this approach. Genetic ablation of MARPs 1-3 blocks the hypertrophic response, although single knockouts are more variable, suggesting extensive complementation between these titin binding proteins. Finally, it is found through the administration of rapamycin that the mTOR signalling pathway plays a role in longitudinal hypertrophic growth.

Strengths:

This paper is well written and uses an impressive suite of genetic mouse models to address this interesting question of what drives longitudinal muscle growth.

Weaknesses:

While the findings are of interest, they lack sufficient mechanistic detail in the current state to separate cross-sectional versus longitudinal hypertrophy. The authors have excellent tools such as the RBM20 model to functionally dissect mTOR signalling to these processes. It is also unclear if this process is unique to the diaphragm or is conserved across other muscle groups during eccentric contractions.

https://doi.org/10.7554/eLife.107597.2.sa1

Author response:

The following is the authors' response to the original reviews.

> ***eLife Assessment***
>
> *The study presents important insights into the regulation of muscle hypertrophy, regulated by Muscle Ankyrin Repeat Proteins (MARPs) and mTOR. The methods are overall solid and complementary, with only minor limitations. Overall, the findings will be of interest for both muscle-biology specialists and the broader mechanobiology community.*

We thank the editors for their interest in our manuscript. Below we respond to the reviewer's comments. Based on these comments we made extensive textual revisions throughout the manuscript, and we added additional analyses to the revised results.

> ***Reviewer #1 (Public review):***
>
> *Summary:*

> *In this manuscript, the authors employ diaphragm denervation in rats and mice to study titin-based mechanosensing and longitudinal muscle hypertrophy. By integrating bulk RNA-seq, proteomics, and phosphoproteomics, they map the stretch-responsive signalling landscape, uncovering robust induction of the muscle-ankyrin-repeat proteins (MARP1-3) together with enhanced phosphorylation of titin's N2A element. Genetic ablation of MARPs in mice amplifies longitudinal fibre growth and is accompanied by activation of the mTOR pathway, whereas systemic rapamycin treatment suppresses the hypertrophic response, highlighting mTORC1 as a key downstream effector of titin/MARP signalling.*
>
> *Strengths:*
>
> *The authors address a clear biological question: "how titin-associated factors translate mechanical stretch into longitudinal fibre growth" using a unique and clinically relevant animal model of diaphragm denervation. Using a comprehensive multiomics approach, the authors identify MARPs as potential mediators of these effects and use a genetic mouse model to provide compelling evidence supporting causality. Additionally, connecting these findings to rapamycin, a drug widely used clinically, further increases the relevance and potential impact of the study.*

We thank the reviewer for their kind words and critical review of our manuscript. The roles of the MARP proteins are diverse and form an intriguing target for further study.

> *Weaknesses:*
>
> *There are several areas where the manuscript could be substantially improved.*
>
> *(1) The statistical analysis of multi-omics data needs clarification. Typically, analyses across multiple experimental groups require controlling the false discovery rate (FDR) simultaneously to avoid reporting false-positive findings. It would be very helpful if the authors could specify whether adjusted p-values were calculated using a multi-factorial statistical model (e.g., ~group) or through separate pairwise contrasts.*

We agree with the reviewer that the description of the statistical analysis could be improved. We report the q-values in the supplemental data tables to correct for false positive data, the p-values reflect pairwise comparisons. Statistical testing was performed on whole proteomes or phospho-proteomes, making for very stringent testing (please also see reply to reviewer 2, response 5). Unbiased quantitative proteomics functions primarily as a screen, in-solution digestion of muscle proteins yields comparatively few peptides making population adjusted p-value calculation very stringent, suggesting no/few differences in expression. Hence, we compared RNAseq to proteome data to isolate consistently differential proteins. We have revised the method section (lines 745-746) to include clarifications of the FDR analysis.

> *(2) (A)There are three separate points regarding MARP3 that could be improved. First, the authors report that MARP3-KO mice exhibit smaller increases in muscle mass after diaphragm denervation compared to wild-type mice (a -13% difference), indicating MARP3 likely promotes rather than attenuates hypertrophy. However, the manuscript currently states the opposite (lines 215-216); this interpretation should be revisited. (B) Second, it would be valuable if the authors could provide data showing whether MARP3 transcript or protein levels change response to denervation - if they do not, discussing mechanisms behind the observed phenotype would help clarify the findings. (C) Finally, given that some MARP-KO mice already exhibit baseline differences, employing and reporting the full two-way ANOVA (including genotype × treatment interaction) would allow a direct statistical assessment of whether MARP deficiency modifies the muscle's response to stretch. This analysis would help clearly resolve any existing ambiguity.*

(A) Compared to wildtype mice, MARP3 KO mice exhibit baseline diaphragm hypertrophy. This suggests that MARP3 may normally restrain hypertrophy under basal conditions. However, in response to UDD, MARP3 KO mice display an attenuated hypertrophic response, which could be interpreted as MARP3 promoting hypertrophy under stress conditions, as noted by the reviewer. The relationship between MARP3 and metabolism remains incompletely understood, but prior studies indicate that loss of MARP3 enhances glucose tolerance and insulin sensitivity (PMID: 12456686), suggesting that MARP3 may act as a negative regulator of metabolic signaling. Both glucose and insulin can activate the PI3K pathway to promote hypertrophy (PMID: 16679293), which may contribute to the baseline hypertrophy observed in MARP3 KO diaphragms. In addition, MARP3 deficiency has been associated with activation of AMPK signaling (PMID: 26398569). AMPK is a key regulator of metabolic pathways and a well-established inhibitor of hypertrophic signaling, in part through suppression of mTOR activity, and is also responsive to mechanical stimuli (PMID: 18556591). Thus, increased AMPK activity in MARP3 KO mice may limit hypertrophy in response to UDD. Supporting this, our phospho-proteomics data indicate increased activation of the AMPK β-subunit following UDD, suggesting a potential role for AMPK signaling in stretch-induced hypertrophy. Based on these considerations, we have removed the statement that MARP3 attenuates hypertrophy and instead incorporated the potential role of AMPK signaling into the Discussion (lines 354–355). While the present study focuses on the triple MARP KO model, future work will examine the specific contributions of individual MARP proteins to muscle hypertrophy.

(B) MARP3 (Ankrd23) upregulation at the RNA level was detected by RNA-seq in rat diaphragm following both UDD and BDD (Supplemental Tables 1 and 2). This is consistent with our prior findings in mice, where western blot analysis showed increased MARP3 protein expression following UDD (PMID: 29978560). We note that reliable detection of MARP3 protein remains technically challenging due to limited availability of specific antibodies.

(C) We agree with the reviewer and have added the results of the two-way ANOVA to the figures (see updated Figure 4). The three MARP proteins exhibit differential effects on diaphragm hypertrophy, supporting their role as modulators of stretch-induced hypertrophy.

> *(3) The current presentation of multi-omics data is somewhat difficult to follow, making it challenging to determine whether observed changes occur at the transcript or protein level due to inconsistent gene/protein naming and capitalization (e.g., proper forms are mTOR, p70 S6K, 4E-BP1). Clearly organizing and presenting transcript and protein-level changes side-by-side, especially for key molecules discussed in later experiments, would make the data more accessible and provide clearer insights into the biology of titin-mediated mechanosensing.*

We agree with the reviewer that naming conventions between gene and protein can be hard to follow. We kept the names for titin-associated proteins as some have multiple protein names and the most common names is shown here. However, we made the suggested changes for the mTOR related proteins (for example, see figure 5).

> *(4) The current analysis relies on total protein measurements downstream of mTOR, yet mTOR's primary mode of action is to change phosphorylation status. Because the authors have already generated a phosphoproteomic dataset, it would be very helpful to report - or at least comment on - whether known mTOR target phosphosites were detected and how they respond to denervation and rapamycin. Including even a brief summary of canonical sites such as S6K1 Thr389 or 4E - BP1 Thr37/46 would make the link between mTOR activity and hypertrophy much clearer.*

We agree with the reviewer that the mTOR data requires more work to ascertain its function in regulating hypertrophy following UDD. We investigated S6K1 Thr389 or 4E BP1 Thr37/46 in both the phosphoproteomic dataset and by western blot. These sites do not appear in phosphoproteome mass spectrometry (supplemental data table 13) and 4E BP1 Thr37/46 was unchanged by western blot (not shown). The S6K1 Thr389 antibody was aspecific in our hands, but Norrby et al (PMID: 22657251) saw increased levels by 6-days UDD. Hence the mTOR aspect of this study is quite complex, suggesting mTOR plays a major role in UDD hypertrophy, but potentially through an alternative activation pathway from what is classically described for muscle hypertrophy. We are investigating the mTOR mechanism further focusing on mTOR's role in regulating longitudinal hypertrophy with potential connection to titin signaling and hope to publish this in the next few years. We revised the discussion to include canonical mTOR activation in hypertrophy, please see lines 388-392.

> *(5) Finally, since rapamycin blocks only a subset of mTOR signalling, a brief discussion that distinguishes rapamycin-sensitive from rapamycin-insensitive pathways would be valuable. Clarifying whether diaphragm stretch relies exclusively on the sensitive branch or also engages the resistant branch would place the results in a broader mTOR context and deepen the mechanistic narrative.*

We agree with the reviewer that distinguishing between rapamycin-sensitive and -insensitive mTOR signaling adds useful context to the interpretation of stretch-induced hypertrophy. Rapamycin primarily inhibits mTORC1, whereas mTORC2 is generally considered rapamycin-insensitive, although prolonged or high-dose exposure can also affect mTORC2 activity. Our data indicate that UDD induces a form of hypertrophy that is sensitive to rapamycin, supporting a prominent role for mTORC1 in this process. However, we cannot exclude the possibility that rapamycin-insensitive pathways, including mTORC2 signaling, also contribute. Notably, denervation itself may influence mTORC2 activity, which could complicate the distinction between stretch- and denervation-mediated signaling. Given these considerations, we have added a brief discussion to acknowledge potential contributions of rapamycin-insensitive mTOR signaling (lines 379-384). A more comprehensive dissection of mTORC1 versus mTORC2 signaling in this context will require targeted approaches and falls beyond the scope of the present study.

> ***Reviewer #1 (Recommendations for the authors):***
>
> *Minor comments:*
>
> *(6) The manuscript notes that KEGG analysis "confirmed" the GO-term findings. Because KEGG pathways and GO terms describe different types of biological information, it might be clearer simply to present them as complementary lines of evidence rather than one validating the other.*

We agree and modified the text accordingly. "Concurrently, KEGG PATHWAY database searches (Supplemental data Table 6) indicated that the DEG's are involved in muscle remodeling." See lines 166-169.

> *(7) Figure 2's legend mentions a two-way ANOVA, but the specific factors tested are not specified. Listing those two factors would help readers interpret the statistics more easily.*

The two-way ANOVA refers to the violin plot in figure 2E and tests the difference of the 2 surgical modalities sham vs UDD and sham vs BDD. Sham groups were combined in the graphs for easy comparison. We clarified the text of figure legend 2.

> *(8) The Methods briefly describe phosphopeptide enrichment, but additional details on the criteria for site identification - such as the localisation algorithm, probability cut-off,*

> *and FDR thresholds - would make the phosphoproteomics section more transparent and reproducible.*

Please see the updated method section, lines 756-765

> ***Reviewer #2 (Public review):***
>
> *Summary:*
>
> *Muscle hypertrophy is a major regulator of human health and performance. Here, van der Pilj and colleagues assess the role of the giant elastic protein, titin, in regulating the longitudinal hypertrophy of diaphragm muscles following denervation. Interestingly, the authors find an early hypertrophic response, with 30% new serial sarcomeres added within 6 days, followed by subsequent muscle atrophy. Using RBM20 mutant mice, which express a more compliant titin, the authors discovered that this longitudinal hypertrophy is mediated via titin mechanosensing. Through an omics approach, it is suggested that the Muscle ankyrin proteins may regulate this approach. Genetic ablation of MARPs 1-3 blocks the hypertrophic response, although single knockouts are more variable, suggesting extensive complementation between these titin binding proteins. Finally, it is found through the administration of rapamycin that the mTOR signalling pathway plays a role in longitudinal hypertrophic growth.*
>
> *Strengths:*
>
> *This paper is well written and uses an impressive suite of genetic mouse models to address this interesting question of what drives longitudinal muscle growth.*

We appreciate the reviewer's kind words on our manuscript and their critical review of our work. A potential separate mechanism governing cross-sectional versus longitudinal hypertrophy is of great interest and something we aim to address in future manuscripts.

> *Weaknesses:*
>
> *While the findings are of interest, they lack sufficient mechanistic detail in the current state to separate cross-sectional versus longitudinal hypertrophy. The authors have excellent tools such as the RBM20 model to functionally dissect mTOR signalling to these processes. It is also unclear if this process is unique to the diaphragm or is conserved across other muscle groups during eccentric contractions.*
>
> ***Reviewer #2 (Recommendations for the authors):***
>
> *(1) Cross-sectional hypertrophy characterization: The paper emphasizes longitudinal hypertrophy but does not quantify the contribution of radial (cross-sectional) hypertrophy to the total mass increase. Given that the denervated costal diaphragm shows ~50% increase in mass (Figure 1B) but there is only ~30% fiber lengthening, it is important to determine the proportion attributable to fiber diameter changes. Histological analysis of muscle fiber cross-sectional area would clarify the relative contributions of longitudinal versus radial hypertrophy to the overall mass phenotype.*

We agree with the reviewer that radial hypertrophy is an important mechanism for muscle weight gain in UDD. In previous work we characterized both the radial and longitudinal hypertrophy response in 6-day UDD and found that ~20% of the mass gain seen in UDD is radial hypertrophy (PMID: 29978560). We reference this paper in the discussion section, line 277-278. Doing a full histological work-up of UDD diaphragm would be interesting but falls outside the scope of this manuscript. Our focus was to characterize longitudinal hypertrophy by addition of sarcomeres in series and provide insight into titin's role in regulating longitudinal hypertrophy. We hope that the reviewer agrees with this approach.

> *(2) Titin isoform expression analysis: At line 103, the authors propose that longitudinal hypertrophy reduces strain on titin by decreasing fractional sarcomere extension. However, this hypothesis does not exclude the possibility of isoform switching to a less elastic titin variant, which may compensate for changes in mechanical stress. The RNA-sequencing data should be analyzed for titin exon usage patterns between sham and UDD to determine whether changes in isoform composition (e.g., PEVK region splicing) accompany longitudinal hypertrophy. If isoform switching occurs, this represents an alternative or complementary mechanism to sarcomere addition.*

We analyzed titin exon usage in rat following both UDD and BDD. Increases in sarcomeres in series associated with UDD show modest changes in titin exon usage, though not significant by population adjusted p-values. The denervation effect of BDD did show changes in splicing, indicating lower inclusion of PEVK encoding exons, suggesting a stiffening of the titin molecules. Stiffening of titin molecules might be protective for the fully paralyzed diaphragm and preserve muscle mass. This would align with our prior publication (PMID: 29978560) which showed that stiffer titin generated more radial hypertrophy in response to UDD. In response to the reviewer's comment, we added the splicing data to the supplemental data as new figure 2 and briefly address titin splicing in the results section, see lines 121-125.

> *(3) The comparison of 3-day unilateral diaphragm denervation (UDD) and bilateral diaphragm denervation (BDD) in rats (Figure 1D-E) is used to argue that hypertrophic signaling is stretch-dependent rather than denervation-dependent. However, this interpretation requires clarification. In mice, hypertrophy is detectable as early as 1 day post-UDD, whereas the 3-day BDD protocol may drive an accelerated hypertrophic-to-atrophic remodelling process given the severity of the model. Moreover, longitudinal and global muscle hypertrophy may operate through distinct mechanisms: denervation could suppress longitudinal hypertrophy through a separate pathway while promoting or delaying cross-sectional hypertrophy. The authors should acknowledge that the current evidence does not fully exclude denervation-dependent mechanisms and should consider extended BDD time points or additional mechanistic studies to clarify this distinction.*

UDD and BDD are both denervation models and hypertrophy occurs in the denervated costal of UDD operated animals. Stretch is thus the mechanical difference between UDD and BDD and thus the trigger for hypertrophy signaling. At the denervation signaling level both models should in principle be comparable and are unlikely to play different roles between UDD and BDD, except that UDD also induces a more potent hypertrophy signaling profile on top of the atrophy program. That said, BDD is a more severe model and respiration rate is depressed compared to UDD where respiration rate is elevated. BDD rats also engage in abdominal breathing, which mildly stretches the diaphragm. Hypoxia is likely to play a stronger role in BDD than UDD and could thus further enhance the atrophy profile of BDD. We agree with the reviewer that more work is needed to elucidate the BDD remodeling response, however UDD induced stretch is the main driver of longitudinal hypertrophy. In response to the reviewer's comment, we have added clarifying text to the discussion, lines 286-292.

The potential for there being two independent mechanisms for both radial and longitudinal hypertrophy is of great interest to us. We foresee that dissecting out these differences will require a cell culture-based approach and will aid in avoiding the complexity of overlapping denervation and hypertrophy signals as seen in this manuscript.

> *(4) Characterization of RBM20 models: The RBM20 experiments rely on the assumption that increased titin compliance reduces stretch sensitivity. However, the paper provides minimal baseline characterization of the diaphragms. Specifically: (a) What are the sarcomere lengths in RBM20-deficient diaphragms at rest and under stretch? (b) How does the passive force-length relationship differ between wildtype and RBM20-deficient diaphragm muscles? and (c) Would RBM20-deficient muscles, despite having longer*

> *sarcomeres at baseline, actually experience sufficient strain to activate mechanosensing? These data are necessary to interpret why RBM20-deficient mice show attenuated mass gain rather than none (as in BDD) during UDD (Supplemental Figure 2A-C). Additionally, what would the authors hypothesize would happen if rapamycin were used in RMB20 UDD models? It appears to be an attractive experimental approach to separate potential mTOR contributions to longitudinal versus cross-sectional hypertrophy.*

We agree with the reviewer that more work is needed on Rbm20 deficient mice and rats to elucidate their response to stretch. Part of this characterization has previously been published (PMID: 29978560) and Rbm20 splice-deficient mice have reduced passive stiffness in the diaphragm and show a robust mechanosensing response to UDD. Rbm20 splice-deficient mice also show a similar increase in longitudinal hypertrophy, but a blunted radial hypertrophy in response to 6-days UDD. The main reason for not expanding on these mice/rats further was the added complexity of Rbm20 splicing multiple targets that could affect hypertrophy signaling, for example LDB3 (ZASP) and FLNC (Filamin C) are both associated with hypertrophic cardiomyopathy. Hence for the purpose of this manuscript we showed mice and rats having a similar response to UDD, hypertrophy wise, and that titin stiffness (reduced in Rbm20-deficient animals) affects hypertrophy at the diaphragm mass level.

Testing rapamycin on Rbm20-deficient animals could be interesting, however the complexities of also changing splicing of non-titin targets will make interpretation of mTOR signaling difficult. Perhaps an alternative approach would be to generate a titin mouse model with more compliant titin (e.g. increase the size of the PEVK segment), a model we are considering for future studies. TtnΔ112-158 mice, deleting a large portion of the PEVK region (PMID: 30565562) show increases in sarcomere number. We would expect a model with more PEVK to thus show a reduction in the number of sarcomeres in series. We discuss the role of titin stiffness in the discussion and how titin stiffness ties to longitudinal hypertrophy, please see lines 302-314.

> *(5) Statistical analysis and multiple hypothesis correction: The proteomic analyses appear to employ a nominal p-value threshold ($p < 0.05$) without correction for multiple comparisons or false discovery rate (FDR) control. This is particularly concerning given the large number of comparisons. For example, the authors report 142 titin phosphorylation sites significantly different between sham and UDD at $p < 0.05$ (approximately 20% of ~700 identified sites). However, with proper FDR correction (adjusted $p < 0.05$), only 14 sites remain significant - a 90% reduction. This discrepancy is critical for the discussion on titin N2A phosphorylation sites pS9459 and pS9520, where only pS9520 achieves statistical significance after FDR adjustment. The authors should justify their choice of statistical thresholds and reanalyze key findings using FDR-corrected p-values. Additionally, the phosphoproteomics dataset should be screened for duplicate phosphosite identifications to ensure each site is counted only once.*

Reviewer 1 has voiced similar concerns, and we have thus expanded the methodology to explain the statistical tests used to analyze the data and the process of establishing Z-scores of isobaric peptides for the same phospho-sites (see lines 756-765). Our statistical analysis covers all detected peptides, when we only analyze the titin peptides: pS9459 is only significant in t-test, likely due to large variation in isobaric peptides. pS9520 is significant in both independent t-test and FDR. We changed figure 3D to show the fold change instead of the previous Z-score for more intuitive interpretation.

> *Minor comments:*
>
> *(6) Line 52: "thesarcomeres" should read "the sarcomeres".*

A space has been added, please see line 52.

> *(7) Line 52: "half-sarcomer" should read "half-sarcomere"*

Spelling has been corrected, please see line 52.

> *(8) Figure clarity: Figure 1 (B-C) presents mouse data, while Figure 1 (D-E) presents rat data. This distinction should be clearly labeled in the figure legend or on the axes to prevent misinterpretation, particularly for readers unfamiliar with the experimental design.*

We added the species to the y-axis of revised figure 1B-E and added additional clarification in the figure legend.

> *(9) Supplementary tables: When reporting statistical comparisons in the supplementary tables, please consider including the directionality of the statistical tests (e.g., which group was higher or lower) alongside p-values. This will facilitate interpretation without requiring reference to the main text figures.*

We agree with the reviewer and added statistical direction as a new column next to the p-values, please see the revised supplemental tables.

> *(10) Given the interesting divergent findings in MARPtKO versus single knockouts, it would be interesting to assess by immunofluorescence the association of each MARP with the N2A region of titin following UDD.*

We agree with the reviewer that localization is important. Miller et al (PMID: 14583192) previously localized MARP1-3 to the N2A segment by immuno-EM and our work previously localized MARP1 to N2A using SR-SIM (PMID: 29978560). We will further investigate MARPs binding to the N2A region in an upcoming study that we intend to publish soon.

https://doi.org/10.7554/eLife.107597.2.sa0